PARSEC

Plume Additive for Reducing Surface Ejecta and Cratering
2024 Human Lander Challenge Technical Paper
Embry-Riddle Aeronautical University

David Clay
Project Manager
Aerospace Engineering
Undergraduate
clayd6@my.erau.edu

Bruce Noble
Deputy Project Manager
Aerospace Engineering
Undergraduate
nobleb2@my.erau.edu

Aidan Kihm
Finance Officer
Mechanical Engineering
Undergraduate
kihma1@my.erau.edu

Jakobe Denby
Safety Officer
Aerospace Engineering
Undergraduate
denbyj@my.erau.edu

Grant Bowers
Testing Officer
Software Engineering
Undergraduate
bowersg3@my.erau.edu

Sanaya Nichani
Media Officer
Aerospace Engineering
Undergraduate
nichans1@my.erau.edu

Dr. Siwei Fan
Faculty Mentor
Dept. Aerospace Engineering
fans2@erau.edu
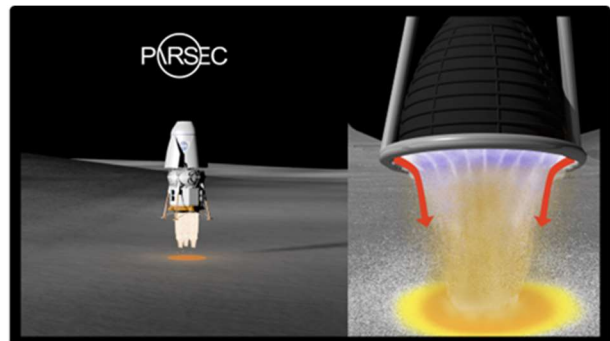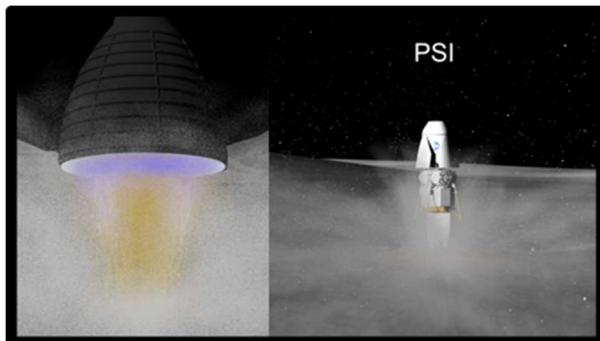
To the HuLC Project Lead: I, _Siwei Fan_____, hereby attest that I have reviewed and approved the proposal submission for the project, titled,

Plume Additive for Reducing Surface Ejecta Cratering, from _Embry-Riddle Aeronautical University_____.
     (project title)   (university)

By signing below, I verify that the submitting team has fulfilled the requirements for my review of the final proposal for the Human Lander Challenge (HuLC) competition. I understand that the electronic signature appearing on this document is the same as a handwritten signature for the purposes of validity and admissibility.

_____   _____
            (signature)   June-3-2024
                                                            (date)

Table of Contents

Table of Tables

Table of Figures

Table of Acronyms

Acronym	Definition
BPP	Baseline Project Plan
CDR	Critical Design Review
CER	Cost Estimating Relationship
COPV	Composite Overwrapped Pressure Vessel
ERE	Employee Related Expenses
FPC	First Pound Cost
FRR	Flight Readiness Review
FY	Fiscal Year
GN2	Gaseous Nitrogen
JSC-1A/F	Lunar mare regolith simulant developed by Johnson Space Center
LM	Lunar Module
LSP-2	Lunar South Pole simulant made by Space Resource Technologies
MCR	Mission Concept Review
NASA	National Aeronautics and Space Administration
NIA	National Institute of Aerospace
ORR	Operational Readiness Review
PARSEC	Plume Additive for Reducing Surface Ejecta and Cratering
PCEC	Project Cost Estimating Capability
PDR	Preliminary Design Review
PPE	Personal Protection Equipment
PPP	Preliminary Project Plan
PSI	Plume-Surface Interactions
SDR	System Definition Review
SiAlON	Ceramic made of Silicon, Aluminum, Oxygen, and Nitrogen
SIR	System Integration Review
SOP	Standard Operating Procedure
SRR	System Requirements Review
TRL	Technology Readiness Level
ZTA	Zirconia-Toughened Alumina

1. **Quad Chart**
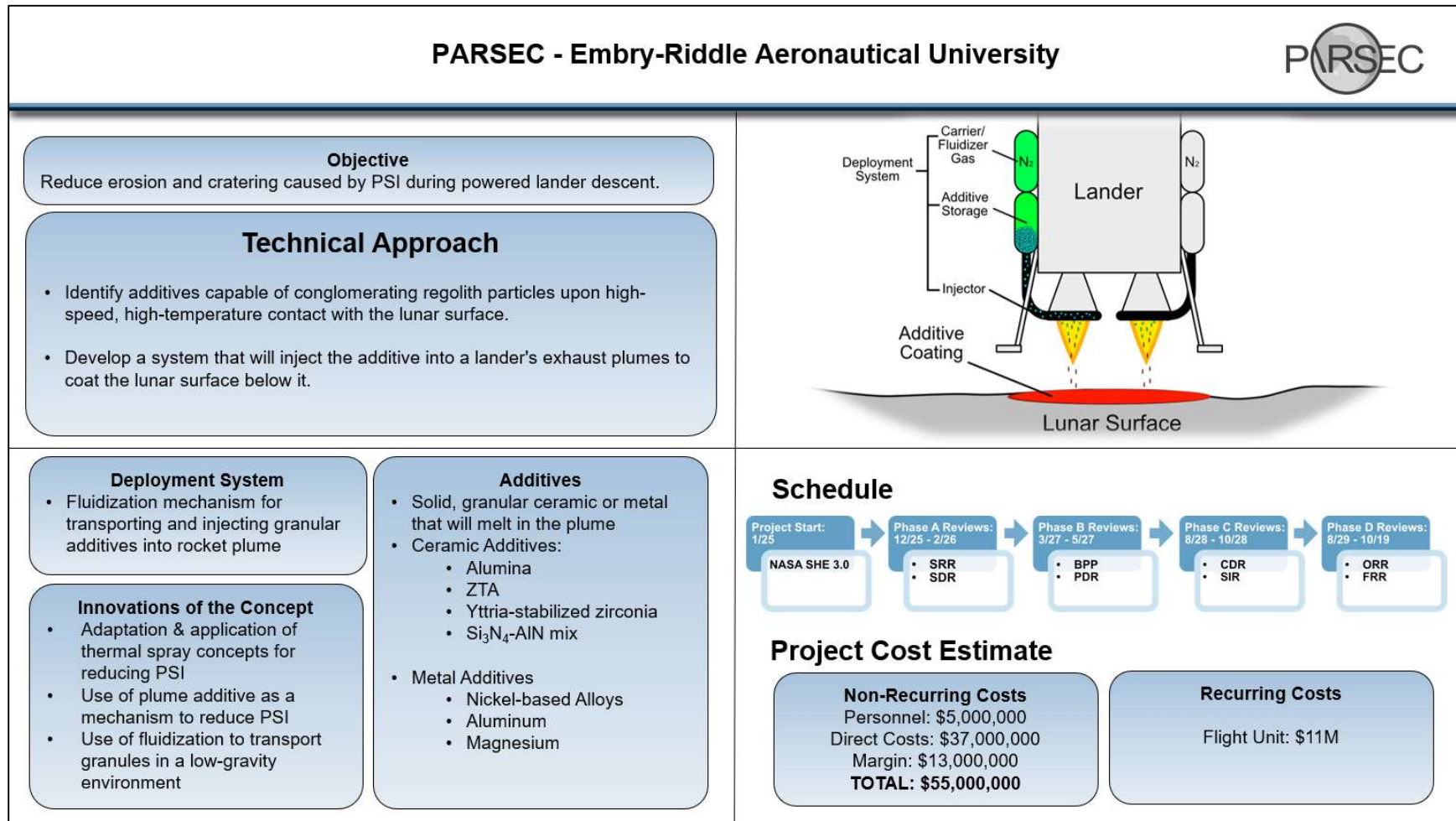
Figure 1 - Quad Chart

2. Technical Paper

2.1. Executive Summary

PARSEC, or Plume Additive for Reducing Surface Ejecta and Cratering, aims to develop an onboard additive-deployment system to mitigate the adverse effects of plume-surface interactions (PSI) from the exhaust plumes of lunar landers. Utilizing concepts of thermal spraying technology, the proposed system will create a temporary landing pad below the lander to increase the stability of the landing site. The pad will be deployed by using a fluidization process; a granular additive will be injected into the exhaust plume of a lander's engine during descent. Upon injection, the additive will begin to melt and accelerate towards the lunar surface, conglomerating the lunar regolith below and solidifying to form a landing pad. Applying this coating to the surface below the lander will reduce the amount of cratering and ejecta that would otherwise occur.

2.2. Problem Statement

During powered descent on the Moon, engine exhaust interacts with lunar soil through heat and momentum exchange, blowing dust radially out from the landing site and producing high-speed ejecta. These particles, ranging from sub-microns to a few centimeters in diameter, can reduce the visibility of sensors and optics, sandblast nearby lunar assets, and erode the surface around the vehicle (Metzger et. al., 2011). The Surveyor III rover, for instance, was positioned in a crater approximately 155 meters from the Apollo 12 landing site. Analysis of the Surveyor III components brought back by astronauts revealed pitting and cracking caused by the spray of dust traveling over 300 m/s from the lander (Immer et. al., 2010). Additionally, particles can be ejected upwards from the surface and create deep craters beneath the lander. This can damage on-board assets and compromise the stability of the landing site (Figure 2). Furthermore, it was reported that Change'e-3 spacecraft which has a total mass of 1.3 metric tons, can create a blast zone with an area of 2530 m^2 during its landing (Clegg-Watkins et al., 2016). Given the size of the landers to be used in the Artemis missions, their blast zones will be much larger than that of Change'e-3, meaning a much more adverse effect will be created from the induced PSI (Watkins et al., 2021). Therefore, to conduct safe landings and establish sustainable exploration on the Moon, it is crucial to understand and mitigate the effects of PSI.
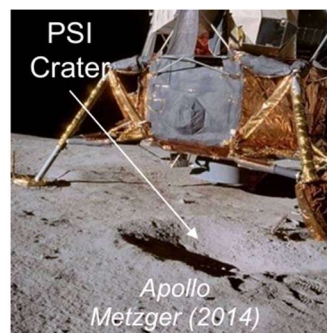
Figure 2 – Cratering on Apollo 12 LM (Korzun & Mehta, 2021)

2.3. Solution

PARSEC proposes a solution capable of mitigating the effects of PSI through the reduction of ejecta and cratering. This aligns with the category outlined in the *2024 Proposal Guidelines for the Human Lander Challenge* titled "Reduction / Mitigation of Erosion (Cratering) and Ejecta during Descent, Landing, and Ascent" (NIA, 2023). The proposed solution will consist of a minimally invasive system installed near a lunar lander's engine nozzles. This device will be capable of storing, transporting, and injecting a granular ceramic or metal additive into each nozzle's exhaust plume. After being melted by the plume, particulates

6

of the additive would adhere – or conglomerate – the regolith to form a solid, composite coating that will serve to shield the lunar surface from the plume and prevent erosion.

2.4. Changes From Proposal

The biggest change PARSEC has made is conducting a set of hot-fire tests on a testbed of lunar regolith simulant, LSP-2, to determine if 4 – 7-micron and 70-micron diameter alumina particles are viable additive options. As the result from a trade study evaluating various additives feasible for testing, accounting for factors such as cost-effectiveness, usability, and transportation, alumina was selected as the preferred additive. Additionally, a nickel alloy was also tested to be effective (see Section 2.5.1.3). This alloy was not originally considered in the proposal, it arrived with the thermal spray torch specifically meant to build up layers on surfaces, thus the team decided to implement it in the test sequence.

In terms of risk management, the initial apprehension regarding Risk 1 (Table 12) – the concern of potential failure of conglomeration – has been addressed, seeing as the testing process showed multiple successful conglomerated pads. In response to feedback from the proposal, additional risks have been incorporated into risk management, including concerns over whether the resulting pad will be destroyed by the plume (Table 12, Risk 3) and if the mass of the additive is too high (Table 12, Risk 2). Tabulated in Table 12, risks were reorganized based on their importance and causal factors, namely additive-induced, deployment-related, and space environment-associated risks.

Another change following the proposal was new mass estimates, which have been reflected in a budget revision. A new analysis of the additive candidates has been conducted, leading to the addition of a new additive which PARSEC tested: a nickel alloy, which was tested alongside Alumina.

2.5. Innovation

2.5.1. Additives Overview

The resulting in-situ landing pad must possess material properties that will allow it to withstand the harsh lunar environment and the landing itself. To survive the intense pressure and shear stresses exerted by the plume – which have been simulated to exceed 32 kPa and 7 kPa respectively for a 40-ton lander – the landing pad material must have a high shear strength, tensile strength, and fracture toughness (Fontes et. al., 2022). The landing pad material must also have a high thermal shock resistance to survive the transition from being subjected to the heat of the lander's exhaust to the cold lunar environment. With the guidance of these requirements, a trade study (Table 10) was conducted to identify plume additives and the decision was made to focus on three forms of additive interactions with the regolith: (1) deploying ceramic or metal particulates that will liquify in the plume and fuse with regolith particles to form a composite on the lunar surface; (2) deploying two nitride ceramics with the intent of causing a physical reaction with the regolith to produce a composite ceramic known as SiAlON; and (3) deploying metal reactants with the intent of causing a thermite reaction to melt the regolith into a composite ceramic.

Using the heat and pressure of the lander's exhaust plume, a coating of ceramic material could be deployed on the lunar surface through a method similar to the industrial process known as thermal spraying. Thermal spraying is a technique that forms protective coatings by accelerating molten or semi-molten particles towards a substrate (Latka et al., 2020). By using the heat and velocity provided by the lander's exhaust plume, it may be possible to replicate this process at a much larger scale to form a temporary landing surface on the Moon.

An ideal additive for this application should have a low density and a high tensile strength to maximize effectiveness. Additionally, the additive should have a melting point below the temperature of the plume – which has been simulated to exceed 3000 K – to ensure that the additive particles can melt before impacting the surface (Fontes et. al., 2022). By comparing several common technical ceramics using *Ansys® GRANTA Selector™* (Figure 8 – Figure 23), PARSEC has decided to focus on the following five

candidates due to their desirable properties: alumina, zirconia-toughened-alumina (ZTA), nickel-based alloys, SiAlON, and thermites.

2.5.1.1. Alumina

Alumina is an accessible and lightweight technical ceramic commonly used as a feedstock for thermal spraying. It has a melting point of 2300 K (Figure 9), which is below the simulated plume temperature of a 40-ton lander. It is assumed that larger particle sizes would be beneficial for conglomeration because as they contact the surface, they would cover a larger section, conglomerating more regolith at one time and creating a larger surface area for the next particle to adhere to.

2.5.1.2. Zirconia-toughened-alumina (ZTA)

ZTA is a ceramic composite made of alumina and zirconia, with the weight percentage of zirconia varying between 5% and 20% for thermal spraying applications (Stanford Advanced Materials, n.d.) (Turunen, 2007). The benefits of ZTA include increases in fracture toughness and flexural strength while maintaining a similar density and melting point to pure alumina (Figure 13 and Figure 15). These properties would be useful for maintaining the structural integrity of the landing pad for a longer period than alumina.

2.5.1.3. Nickel Alloys

PARSEC began considering nickel alloys as a potential additive candidate after conducting a series of conglomeration tests in April 2024 using a powder spray torch. These tests resulted in the successful conglomeration of Victor Buildup #22 – a nickel alloy – and LSP-2 – a lunar regolith simulant. Nickel alloys are often used as feedstocks for thermal spraying applications because they can form high bond strength coatings on ceramic or abradable materials (Sanpo et. al., 2013). This could explain why Buildup #22 bonded well with LSP-2, which is effectively a highly abradable ceramic material. A possible advantage these metals would have over ceramics is their higher ductility (Figure 20); this could prevent the landing pad from shattering abruptly into sharp fragments. However, this also means there is possibility of a metal landing pad deforming under the plume's load, which would make it less effective at mitigating cratering. This effect may have been responsible for the parabolic shape of a specimen obtained from spraying Buildup #22 onto a bed of desert sand, as seen in Figure 3.
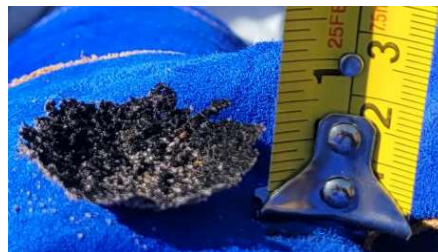
Figure 3 – Parabolic Specimen obtained from Buildup #22 Conglomeration, Test 4

Two more advantages nickel has over ceramics are (1) its high thermal conductivity and (2) low melting point at high purities (Figure 21 and Figure 22). Together, these properties would allow nickel particulates to melt faster in the plume, increasing the likelihood that they will be molten before impacting the surface. Additionally, the high thermal conductivity would allow the nickel to cool faster upon contact with the lunar surface and solidify into a landing pad sooner. However, additional drawbacks of nickel include that it is approximately 50% more dense than zirconia and can cost 50% more than the most expensive ceramic additives, depending on the alloy used (Figure 23). Nickel powders are also suspected of leading to nasal and pulmonary cancer after prolonged exposure, meaning further precautions will need to be taken during handling and storage (Gates, 2023).

2.5.1.4. SiAlON

SiAlON is a ceramic compound formed through the sintering of silicon nitride, aluminum nitride, alumina, and silica with the addition of rare metals such as magnesia (International Syalons, 2021). The material properties of SiAlON were compared with the material properties of various sprayable ceramics (Figure 8 – Figure 19). SiAlON has similar properties to several of the sprayable ceramics, except that it has higher strength and thermal shock resistance (Figure 8, Figure 14, and Figure 15) which may be beneficial for the rapid transition from the loads of the lander to the lunar environment.

The use of magnesia at 10% weight in sintering SiAlON has been shown to effectively produce SiAlON in a variation of the process known as "pressureless sintering", conducted under 5 Pa between 1300 °C (1600 K) and 1500 °C (1800 K) (Mackenzie, 2000). The lunar regolith contains alumina, silica, and magnesia already; with the addition of silicon nitride and aluminum nitride as plume additives, it may be possible to undergo pressureless sintering and form SiAlON as the magnesia replaces portions of the silica in the structure of SiAlON (Yu, 2014). Since silicon nitride and aluminum nitride are common thermal spraying materials, they can be deployed in a similar process to sprayable ceramics with alterations to the deployment angle to ensure the additives reach the 1800 K required for pressureless sintering.

2.5.1.5. Thermite Reactions

Thermite reactions rely on a mixture of aluminum or magnesium with an oxide. When the mixture is heated, the oxygen is stripped from the oxide and reacts with magnesium or aluminum, releasing energy and eventually passing the activation energy needed to sustain the reaction (Delgado, 2013). Because the lunar regolith is composed of mostly oxides, it may be possible to produce a thermite reaction on the lunar surface using deposited heated aluminum or magnesium powder. Experiments conducted using JSC-1A lunar regolith simulant and 10% weight magnesium under an argon atmosphere have demonstrated that a sustained thermite reaction is possible utilizing materials commonly found on the lunar surface (Delgado, 2013).

Thermite was chosen as a viable reaction because a prototype has been developed using nano-thermite microcapsules to help mitigate PSI. Texas A&M Engineering Experiment Station shows that it may be possible to build a regolith solidification system with built-in microcapsule-based welding and iron-based anchors (Hall, 2021). The exothermic reaction that occurs upon deployment allows for simplicity in the creation of a cement-like surface.

2.5.2. Deployment System Overview

For PARSEC to successfully be implemented, a deployment system must be designed to safely store, convey, and inject the additive into the exhaust plume of the lander. The deployer must be lightweight – to not hinder the functionality of the lander – and be able to function in a low gravity environment without experiencing blockages which are common to industrial material storage. By conducting a trade study on possible deployment methods (Table 11), it was decided to develop a design based on two promising models: fluidization and thermal spraying.

The fluidization of powders occurs when a fluid passes through small and uncompacted particles. As the fluid moves between particles, it imparts a drag force on each, moving them while also reducing friction by creating a fluid barrier between the particles (Kaczmarek et al., 2019). This process is currently used in industrial applications such as food processing, chemical engineering, and polymer coating. The current deployer design takes inspiration from industrial fluidizing grain silos: special silo bottoms, such as the Siperm® Fluidization Bottom, are designed with porous materials to allow pressurized gas to be pumped through its walls (Siperm, 2024). This method prevents common problems with the bulk transport of materials such as rat-holing. Rat-holing occurs when a stable bed of powdered material forms from a lack of agitation, and when the storage is emptied, the center of the stable bed shears, removing only the portion of the material directly over the opening (Matchett, 2006). Like the Siperm® Fluidization Bottom,

PARSEC's deployer is systematically lined with openings to pump nitrogen gas into the additive bed. The nitrogen gas will fluidize the additive before deployment and carry the material to the injection nozzle, where it will enter the lander's exhaust plume. Additionally, with fluidization, additives can be stored safely from the heat of the exhaust plume and rapidly transported to the injector.
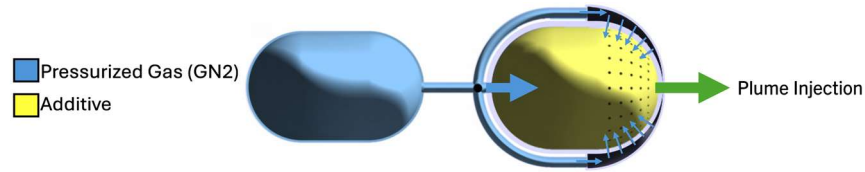
Figure 4 – Deployment System Diagram

Once the additives have entered the exhaust plume, the particles will be heated and accelerated towards the lunar surface. In thermal spraying, materials are heated by an oxygen-fuel mixture and ejected to form a protective layer on the targeted surface (Fan, 2021). Testing needs to be conducted to determine the optimal angle for deployment so that the additives reach the surface at appropriate temperatures. Currently, fluidization has not been documented in low gravity environments, and thermal spraying has not been conducted on uncompacted regolith; thus, limited by time and resources, there are uncertainties in this proposal of our solution.

2.5.3. Technological Assumptions

PARSEC is currently at TRL 3. In April 2024, the team conducted a series of proof-of-concept tests. A nickel alloy (Buildup #22) was successfully thermal sprayed on samples of LSP-2 simulant with attempts made for alumina. To progress to TRL 4, further testing must be done with thermal spraying at higher temperatures to ensure the alumina will melt properly.

2.6. Analysis

2.6.1. Methods for Mitigation

A trade study was used to determine that a plume additive is the most viable mitigation method to pursue (Table 9). This and other possible methods were rated based on selection criteria, including modification to the lander; current understanding of the method; information available on the method; reusability of the method; TRL; size; cost; power requirements; effectiveness in mitigating PSI; complexity of the solution; and safety. The plume additive was chosen as the most effective mitigation method mainly due to its reusability, low power usage, low complexity, and safety.

2.6.2. Conglomeration Tests

In April 2024, PARSEC performed a total of 18 tests, all but two of which utilized additives to prove the validity of the solution proposed to the HuLC team (Table 13). The tested additives were alumina and "Buildup #22" – a nickel alloy manufactured by Victor that is specifically engineered to be compatible with their powder spray oxy-acetylene torch. This torch was used to simulate a scaled down lander plume. The additives – alumina and Buildup #22 – were injected into the torch plume through a built-in feeder mechanism and subsequently deployed onto a bed of powder, intended to simulate the dusty lunar surface. PARSEC conducted a total of two additive tests on a bed of sand and 12 additive tests on a bed of LSP-2, a lunar regolith simulant manufactured by Space Resource Technologies. Out of the 16 additive tests conducted, PARSEC successfully generated and analyzed a total of nine solid formations of conglomerated surface.

Figure 5 –Test 4 with Multiple Camera Angles

2.6.2.1. Alumina Tests

Out of the six original additive candidates outlined in PARSEC's proposal document, alumina was the only one that was testable, given budgetary restrictions and safety constraints. A total of seven tests were conducted on LSP-2 with alumina. One test occurred with alumina sizes of 4-7 µm, while the rest occurred at a size of 70 µm. The only success with alumina occurred during test 9 of the 70 µm size, in which a section of LSP-2 was observed to have conglomerated successfully. This piece proved to be fragile, however, as it broke while being retrieved from the testing section. As a result, the less sturdy parts broke away, where now only a 0.11 cm², non-disc shaped sample remains, which under a microscope still shows conglomeration. PARSEC has deemed the alumina tests as inconclusive, due to issues getting the ceramic particles to flow properly through the thermal sprayer (see Section 2.6.4).

2.6.2.2. Buildup #22 Tests

Buildup #22 was not an additive outlined in the original proposal document, but it was chosen in testing to collect more data. Using this additive, PARSEC consistently generated landing-pad-like formations on the surface of the LSP-2 simulant, creating five of these formations on LSP-2, two on desert sand, and one on a fire brick. 100% of the tests utilizing Buildup #22 generated a conglomerated sample. All the samples collected with this additive were much stronger than that of the alumina and formed solid conglomerated discs of regolith ranging from 3 cm to 6 cm in diameter, depending on the test parameters. PARSEC ran three tests with Buildup #22 set at 14 cm above the LSP-2 surface ranging from 20 to 60 seconds in duration to observe its effects (Figure 24). The most successful of these tests was the 60 second version, which yielded a 6 cm-diameter disc of LSP-2 simulant held together by the additive. Despite the long duration of the burn, the sample remained intact even during exposure to the extreme heat of the torch, giving PARSEC confidence in the proposed solutions' thermal capabilities. For the sand tests utilizing this additive, analysis on the samples showed that the weight composition of the formed pad was approximately 48 wt% additive and 52 wt% desert sand.

This additive is primarily an alloy of nickel and chromium (Victor, 2010). The conglomeration of the test surfaces, promising structural integrity of the retrieved samples, and apparent thermal integrity of the pads has given PARSEC the confidence to deem the Buildup #22 tests as a success. Further observations of these samples underneath a microscope (Figure 6) supported these findings, showing conglomeration of the metallic additive. The demonstration of success of these miniaturized tests operates as a proof of concept for further development of PARSEC's solution on a larger scale.

Figure 6 – Test 17 Sample (Left: 6 cm Diameter, Right: Microscopic Sample Image)

2.6.3. Landing Pad Stress Model

A model based on the rule of mixtures was developed to obtain estimates of the stresses a landing pad would be subjected to upon formation. The model was based on the following assumptions: (1) the landing pad is a solid, particle-reinforced composite composed of anorthosite particulates uniformly distributed throughout a matrix comprised of the additive; (2) the landing pad structure possesses isotropic elasticity; (3) no pores or voids are present within the landing pad structure; and (4) the landing pad structure is governed by the following deflection relationship:

$$\delta_{pad} = \delta_{additive} + \delta_{regolith} \qquad (1)$$

The following equations for the composite elastic modulus and tensile strength were then derived:

$$E_{pad} = \frac{E_{anorthosite}E_{additive}}{v_{anorthosite}E_{additive} + v_{additive}E_{anorthosite}} \qquad (2)$$

$$\sigma_{UTS,pad} = \sigma_{UTS,additive}v_{additive} + \sigma_{UTS,anorthosite}v_{anorthosite} \qquad (3)$$

where E is the elastic modulus, v is the volume fraction, and σ_{UTS} is the ultimate tensile strength. Static structural simulations were conducted in ANSYS® Mechanical® to identify landing pad properties and dimensions required to survive the expected loading conditions. Further details and the parameters of each simulation are provided in the Appendix. Table 1 lists factors of safety obtained for a landing pad of diameter 8 m and thickness 2 cm with different additives and weight percentages. This diameter was selected to be large enough to shield the lunar surface from most of the simulated load exerted by a 40-ton lander on the lunar surface (Fontes et. al., 2022), and this thickness was selected to provide a factor of safety greater than one for all configurations in Table 1. The total mass of additive required for the landing pad depends on the type of additive and weight percentage as shown in Table 1.

Table 1 – Landing Pad Factors of Safety and Masses

Additive	Tensile Stress Factor of Safety				Additive Mass (kg)			
	90 wt%	50 wt%	25 wt%	10 wt%	90 wt%	50 wt%	25 wt%	10 wt%
Alumina	13.6	6.2	3.1	1.6	3280	1410	620	230
Zirconia	54.6	19.5	8.3	3.4	4630	1620	660	240
ZTA	11.9	5.5	2.7	1.4	3350	1430	620	230
SiAlON	22.2	10.7	6.9	3.6	2840	1330	600	230
Nickel Alloy	20.2	6.3	2.8	1.4	6170	1770	680	240

These results suggest that a landing pad of this size will survive the loads exerted by the lander plume if it were composed of 10 wt% additive or greater. If the landing pad were to be composed of 50 wt%

additive, the total mass of additive required would be less than 1800 kg, or 4.5% of the lander mass. This weight percentage was assumed to be sufficient because the factors of safety in Table 1 for all additives are greater than 5, with the factors for SiAlON and zirconia being greater than 10 and nearly 20, respectively.

While the simulations have provided necessary and promising data for this analysis, its inaccuracies must be noted. The rule of mixtures formulas for elastic modulus and tensile strength do not consider other complex factors that may affect these properties, such as the degree of adhesion between the matrix (additive) and particulates (regolith) and the change in matrix properties due to the presence of these particulates (Li et. al., 2001). Additionally, a landing pad formed through this process would be nonuniform in composition and contain many voids and pores. This would result in different tensile strengths than what was estimated and stresses that are higher than those observed in the simulation. Other assumed parameters used in the simulation may also be inaccurate such as: the deformation modulus of the regolith bed, which is shown to heavily influence the maximum stresses of the landing pad in Table 15; and the mechanical and physical properties of anorthosite and the additives, which are shown in Table 14. This simulation also assumes the properties of the landing pad and load are static, which is inaccurate. Physical tests and further analyses are necessary to determine whether the landing pad will remain intact during landing to higher confidence.

2.6.4. Deployment System

A trade study was used to select the design of the deployment system based on trades including the modifications that must be made to a lander (Table 11). Fluidization and COPVs ranked the highest; therefore, they were chosen to proceed with.

The volume of each additive was calculated (Table 2) by dividing the mass taken from 50 wt% Landing Pad Stress Model (Section 2.6.3) by their respective densities (Table 14). While the volume and mass of the deployment system in full could not be calculated, the volume of additive required for the desired pad strength does aid in the approximation.

Table 2 – Volume Requirement for Each Additive

Additive	Volume (m^3)
Alumina	0.36
Zirconia	0.27
ZTA	0.36
SiAlON	0.40
Nickel Alloy	0.20

As fluidization is a large part of the deployment system, the minimum velocity required to fluidize alumina particles at various particle diameters was calculated (Table 3). To do so, the following equations were used where Ar is the Archimedes number, ρ_g is fluid/gas density, d_p is particle diameter, ρ_p is particle/solid diameter, μ is the viscosity of the fluid, and u_{mf} is the minimum fluidization velocity. These equations are based on the Wen and Yu minimum fluidization correlation (Cocco et al., 2014). A density of 1.2506 kg/m^3 was used for GN2 with μ as 0.018 cP.

$$Ar = \frac{\rho_g d_p^3 (\rho_p - \rho_g) g}{\mu^2} \tag{4}$$

$$Ar = (1650)\, Re + (24.5)(Re)^2 \tag{5}$$

$$Re = \frac{(\rho_g)(u_{mf})(d_P)}{\mu} \qquad (6)$$

As the calculated Archimedes number depends upon gravitational acceleration, an assumption was made that the system would experience lunar gravity, as while landing, the lander would ideally hover or descend at a near constant rate making the largest acceleration experienced be that of the Moon itself. Furthermore, these equations assume that the additive particles are completely spherical in shape – which is not feasible. However, the rougher a particle, the less velocity required to fluidize it due to its drag (Cocco et al., 2014).

Despite the popularity and usefulness of Wen and Yu's correlation, it may not be entirely accurate in calculating u_{mf} (Gibson et al., 2018).

Table 3 – Minimum Fluidization Velocities for Alumina

Minimum Fluidization Velocity for Alumina Particles with GN2 Fluid ($g = 1.625$ m/s^2)			
Particle Size d_p (m)	Ar	Re	u_{mf} (m/s)
1 micron 1.0E-06	2.4E-05	1.5E-08	2.1E-07
5 microns 5.0E-06	3.1E-03	1.9E-06	5.3E-06
10 microns 1.0E-05	2.4E-02	1.5E-05	2.1E-05
50 microns 5.0E-05	3.1E+00	1.9E-03	5.3E-04
100 microns 1.0E-04	2.4E+01	1.5E-02	2.1E-03
500 microns 5.0E-04	3.1E+03	1.8E+00	5.2E-02
1 millimeter 1.0E-03	2.4E+04	1.2E+01	1.8E-01
5 millimeters 5.0E-03	3.1E+06	3.2E+02	9.2E-01
1 centimeter 1.0E-02	2.4E+07	9.7E+02	1.4E+00
5 centimeters 5.0E-02	3.1E+09	1.1E+04	3.2E+00
10 centimeters 1.0E-01	2.4E+10	3.2E+04	4.5E+00

While an attempt was made at calculating an estimated mass of the deployment system, it was discovered that sufficient information was not available, and too many incorrect assumptions would have to be made. To continue, either simulations or tests of fluidized beds with selected additives would need to be done to find accurate volume flow rates to determine how much GN2 to use.

While conducting tests with Alumina powder, it was found that the roughness of the particles caused the powder to clog. This issue is commonly solved by fluidizing such powders (Siperm, 2024). If such fluidization were to have been practiced, the alumina particles would not have experienced rat-holing. However, as the Buildup #22 powder was spherical in shape and went through the hopper without any complications, further analysis will need to be done to determine whether spherical powders pose less risk despite their higher minimum fluidization velocity, or whether an optimal ratio of sphericity to minimum fluidization velocity can be found to minimize the risk of not deploying.

2.6.5. Additive Candidates

The leading additive candidates were selected based on a trade study, presented in Table 8. Ceramics, specifically alumina and zirconia, were ranked highest in this study, scoring highest in every category. SiAlON as a standalone was ranked second, with a reduced score in deployment, TRL, and functionality; these reductions were due to its lack of testability in forming within a lunar-adjacent environment.

When mixing with thermites, it was found that aluminum and magnesium are both excellent candidates. As such, a comparison was made between Al and Mg. Prior research shows that a geo-thermite reaction

will occur between JSC-1AF lunar regolith simulant and aluminum powder. (Faierson, 2010) Mg usually ignites at lower temperatures due to lower protection properties of the oxide surface film, and it is thermodynamically advantageous when mixed with lunar regolith. However, in experiments with mixtures at a low pressure of 3300 Pa, due to a high vapor pressure of Mg, gases evolved during the combustion process and the resulting product had significant porosity. When the pressure level was further decreased, the pellet disintegrated. However, this phenomenon was mitigated with a lower vapor pressure of Al (Delgado, 2013).

The ceramics have been shown to have adequate melting temperatures, but it is equally important to have high thermal conductivity, tensile strength, and compressive strength to survive the transition from the heat of the lander's exhaust to the cold lunar environment. Table 4 contains these properties for alumina, ZTA, zirconia, and SiAlON.

Table 4

Table 4 – Ceramic Properties (ANSYS®, Inc.)

Additive	Thermal Shock Resistance (K)	Tensile Strength (MPa)	Compressive Strength (MPa)
SiAlON	620 - 710	400 - 700	3500 – 4500
Alumina (99.95% purity)	342 - 351	247 - 273	2470 – 2730
ZTA (82.5% alumina)	346 - 355	219 - 242	2190 – 2420
Zirconia (yttria-stabilized)	804 - 869	1070 - 1180	10700 – 11800

2.7. Validation and Verification

2.7.1. Validation

The additive-deployment system was not the first solution the team investigated. Preliminary analysis included a trade study, conducted to determine the best approach to the problem, and a plume additive was found to be the most effective solution. Validation of the proposed system has been completed via an integrated system test: alumina as an additive was deployed onto a lunar regolith simulant test bed with the dual objectives of a) promoting the conglomerated formation of regolith particles and b) reducing PSI.

During the testing phase, it became apparent that analyzing PSI would pose challenges due to the absence of a vacuum environment; this rendered it impractical to reliably capture reduction on a camera. However, conglomeration occurred during multiple tests and samples were collected, thereby affirming the system's efficacy in accomplishing its intended requirements (Table 13). Given the limitations in detecting PSI, the next steps would involve implementing specialized testing tailored to measure PSI, using the same additive. The team created this testing process with repeatability in mind, meaning that our steps can be reproduced.

2.7.2. Verification

Through analysis and testing, the team determined the efficacy of PARSEC's solution in promoting the conglomeration of regolith and mitigation of PSI. Initial analysis comprised two trade studies, one determining the chemical additive (Table 10), and the other determining the design of the deployer (Table 11). After further researching and developing the concepts of ceramics and fluidization, the team moved to working with analytical software such as ANSYS® Fluent® and SolidWorks® to model and simulate the additive injection into the lander's plume. For testing, PARSEC developed SOPs to experiment with mixing and thermal spraying four-seven micron and 70-micron alumina onto a test bed of lunar regolith simulant.

Testing verified the team's design and additive choices as conglomeration samples were collected, and analysis with simulations support the solution. Although a clear measurement of PSI reduction was not

taken, as per video observation of the tests, PSI may have been marginally reduced. Due to the difficulty in spotting small particles on video, PARSEC cannot definitively conclude as to whether PSI had been sufficiently impacted. Yet still, half of the team's hypothesis was proven right as the conglomeration aspect was a total success, underscoring the viability of further testing to provide more comprehensive and conclusive results.

2.7.3. Risks

To analyze the risks posed by PARSEC's design, a risks management and matrix sheet was created (Table 12) compiling a total of seventeen relevant risks to determine each risk's concern level and mitigation plans. The results of this analysis posed four high priority risks.

In accordance with testing and feedback from the HuLC competition readers, new risks have been considered (Table 12, Risks 2, 3, and 17). To account for an inconvenient additive mass being brought to the Moon, calculations were conducted for multiple additives based on 50% wt, 25% wt, and 10% wt (See Table 1). For Risk 3, landing pad stress calculations were conducted (See Section 2.6.3). Risk 17 can be mitigated with more testing.

Table 5 – Risk Priority Matrix

LIKELIHOOD		1	2	3	4	5
	5					
	4		7			2,5
	3		9	14	6,17	1,3
	2			15		11
	1	8		16	10,12,13	4
		1	2	3	4	5
				CONSEQUENCES		

The highest priority risk (Table 10, Risk 1) addresses the possibility that the chemical or bonding reactions may never happen, which results in no landing pad being formed. Testing results proved the formation of a solid pad is probable with a thermal spray gun, with a sample of a pad formed in the figure below. However, upscaled testing and more accurate atmospheric conditions will be needed to completely mitigate this risk.
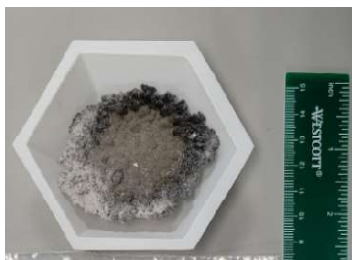
Figure 7 – Buildup #22 60-Second Test 2.25-inch Sample

The thermal dynamics of the plume's interaction with the additive also poses two critical risks (risks 4 and 5). Due to the thermal extremes created by the lander's plume and the lunar environment, the additive may not melt as intended, or may be heated beyond usability. There is little research done on an additive's thermal behavior in a rocket plume in space, so to overcome the severity of this risk, the additive's properties must be evaluated in a thermal simulation software, such as ANSYS® Fluent®.

Another high concern risk is the mass of the system. If the true mass of the system exceeds 5% of the lander's mass, then the system will become more inconvenient than useful (as set in Section 0). Considering this mass criteria, the deployment system has been set to a mass of 200 kg, but the additive mass and tank mass are variable. While there is an estimated required additive mass of 1410 kg (Section 2.6.3, Table 1 for Alumina at 50wt%), many assumptions were made to obtain that ratio, so it is possible the true mass of additive will be higher than expected.

The last high priority risk concerns the strength of the temporary landing pad relative to the force created by the lander's thrust. If the pad yields, larger conglomerated regolith chunks could be ejected, possibly becoming more dangerous. To overcome this risk, the team analyzed the specimens created during testing to reach the hypothesis that the pad will survive the plume by approximating the specimens' elastic modulus and ultimate tensile strength (see Section 2.6.3).

While not as high in priority, the additives and regolith pose respiratory and skin health hazards (Table 10, Risk 8) (Space Resource Technologies, 2021) (GNPGraystar, 2020), which became prevalent when preparing for testing. During the team's testing, engineering controls were put in place to prevent the creation of dust, such as a mobile glove box and appropriate PPE. Additionally, a mobile eyewash station and mobile shower were ready for use if needed. On an industrial scale, similar but industrial-scale safety equipment will be required.

2.8. Budget

Utilizing NASA's Project Cost Estimating Capability (PCEC) software, estimates for both non-recurring and unit costs of the deployment system were derived for a 40-ton lander using a First Pound Cost (FPC) Cost Estimating Relationship (CER). This CER accepts the estimated weight of a system in pounds and inputs it into a formula based on the cost trends of mechanical systems on previous lander-type missions to predict costs for future missions in development (NASA, 2021). A mass of 200 kg (440 lb_m) was used as an input for this estimate, assuming the maximum total mass of the deployment system on a 40-ton lander is 200 kg, excluding the mass of the additive. This assumption is based on a design requirement that the total mass of the system shall not exceed 5% of the total lander mass, where 4.5% (1800 kg) and the remaining 0.5% (200 kg) is allocated to the additive and deployment system, respectively. Section 2.6.3 provides more information on why this additive mass constraint was used. Table 6 contains the cost outputs of the CER and their inflation-adjusted amounts.

Table 6 – PCEC Cost Outputs (Millions of Dollars)

Cost Phase	FY2015 $M (Direct Output)	FY2024 $M (Inflation-Adjusted)
Non-Recurring	19.6	23.3
Design & Development	7.4	8.7
System Test Hardware	12.3	14.6
Flight Unit	9.4	11.2

The non-recurring costs were inflation-adjusted and converted to an annuity distributed across the project life, assuming a 2.6% yearly interest rate. These costs were included along with a 50% manufacturing margin in the total direct costs of the project. Personnel salaries are also included in the overall cost estimate. Travel costs are neglected assuming all personnel will be living in Huntsville, Alabama, and all tests can be conducted at either NASA's Marshall Space Flight Center or Blue Origin's Blue Engine facility.

Table 7 contains a breakdown of the current cost estimate for the project, excluding any changes that may occur to the cost of launching the mission.

Table 7 – Cost Estimate (Thousands of Dollars)

Mission Phase	Phase A	Phase B	Phase B	Phase C	Phase D	
Year	FY 1 (2025)	FY 2 (2026)	FY 3 (2027)	FY 4 (2028)	FY 5 (2029)	Cumulative Total
PERSONNEL						
Science Personnel (1)	80	82	82	86	88	419
Engineering Personnel (4)	320	328	328	345	353	1,675
Technicians (1)	60	62	62	65	66	314
Administration Personnel (2)	120	123	123	129	132	628
Project Management (2)	240	246	246	259	265	1,256
Total Salaries	**820**	**841**	**841**	**884**	**905**	**4,292**
Total ERE	**229**	**235**	**235**	**247**	**253**	**1,198**
DIRECT COSTS						
System Cost (from CER)	4,660	4,781	4,902	5,023	5,145	24,512
Manufacturing Margin (50%)	2,330	2,391	2,451	2,512	2,572	12,256
Total Direct Costs	**6,990**	**7,172**	**7,353**	**7,535**	**7,717**	**36,767**
FINAL COST CALCULATIONS						
Total Projected Cost	8,039	8,248	8,430	8,666	8,880	42,263
Total Cost Margin (30%)	2,412	2,474	2,529	2,600	2,664	12,679
Total Project Cost	**10,451**	**10,722**	**10,958**	**11,266**	**11,545**	**54,941**

2.9. Project Timeline

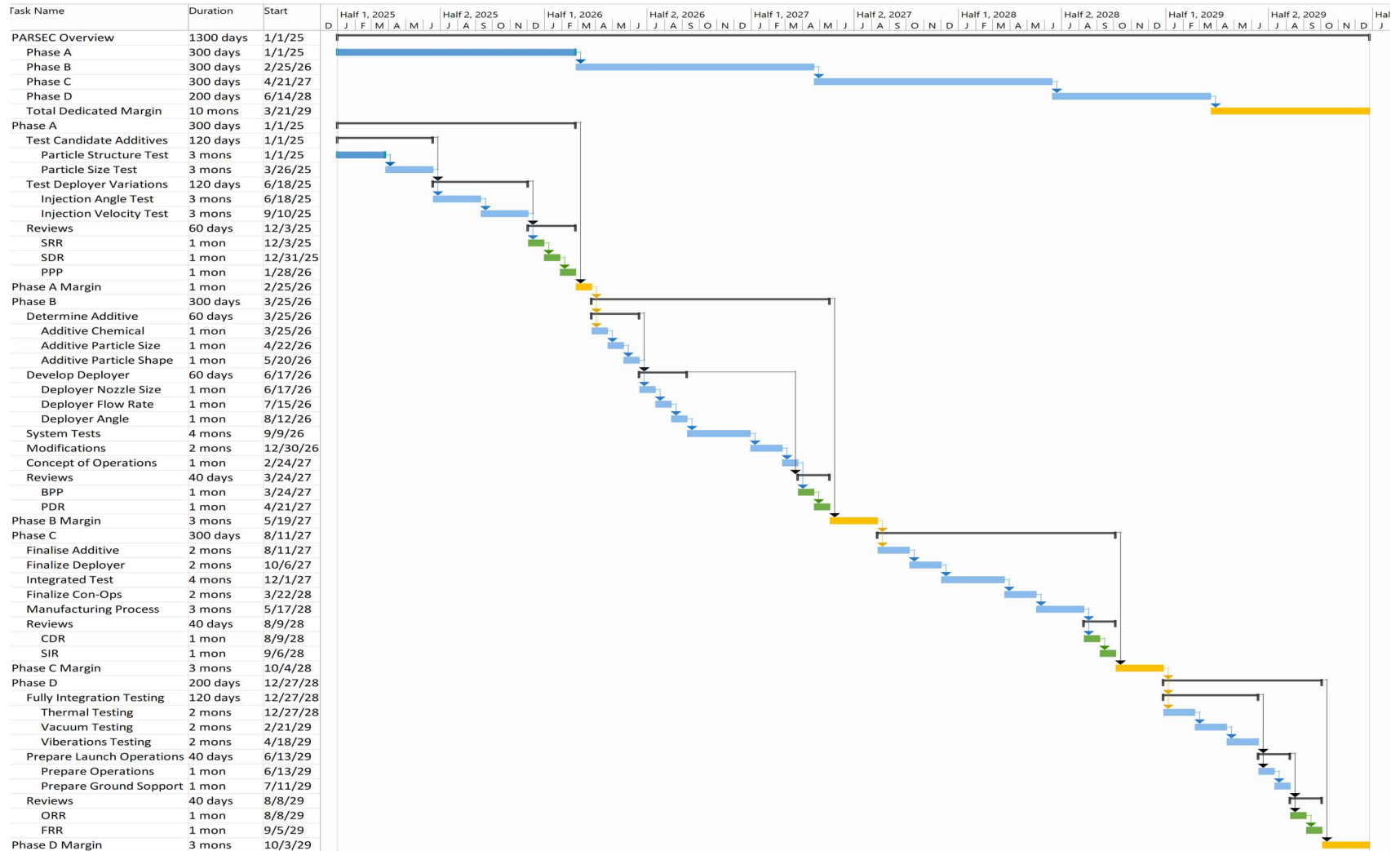| Task Name	Duration	Start
PARSEC Overview	1300 days	1/1/25
Phase A	300 days	1/1/25
Phase B	300 days	2/25/26
Phase C	300 days	4/21/27
Phase D	200 days	6/14/28
Total Dedicated Margin	10 mons	3/21/29
Phase A	300 days	1/1/25
Test Candidate Additives	120 days	1/1/25
Particle Structure Test	3 mons	1/1/25
Particle Size Test	3 mons	3/26/25
Test Deployer Variations	120 days	6/18/25
Injection Angle Test	3 mons	6/18/25
Injection Velocity Test	3 mons	9/10/25
Reviews	60 days	12/3/25
SRR	1 mon	12/3/25
SDR	1 mon	12/31/25
PPP	1 mon	1/28/26
Phase A Margin	1 mon	2/25/26
Phase B	300 days	3/25/26
Determine Additive	60 days	3/25/26
Additive Chemical	1 mon	3/25/26
Additive Particle Size	1 mon	4/22/26
Additive Particle Shape	1 mon	5/20/26
Develop Deployer	60 days	6/17/26
Deployer Nozzle Size	1 mon	6/17/26
Deployer Flow Rate	1 mon	7/15/26
Deployer Angle	1 mon	8/12/26
System Tests	4 mons	9/9/26
Modifications	2 mons	12/30/26
Concept of Operations	1 mon	2/24/27
Reviews	40 days	3/24/27
BPP	1 mon	3/24/27
PDR	1 mon	4/21/27
Phase B Margin	3 mons	5/19/27
Phase C	300 days	8/11/27
Finalise Additive	2 mons	8/11/27
Finalize Deployer	2 mons	10/6/27
Integrated Test	4 mons	12/1/27
Finalize Con-Ops	2 mons	3/22/28
Manufacturing Process	3 mons	5/17/28
Reviews	40 days	8/9/28
CDR	1 mon	8/9/28
SIR	1 mon	9/6/28
Phase C Margin	3 mons	10/4/28
Phase D	200 days	12/27/28
Fully Integration Testing	120 days	12/27/28
Thermal Testing	2 mons	12/27/28
Vacuum Testing	2 mons	2/21/29
Viberations Testing	2 mons	4/18/29
Prepare Launch Operations	40 days	6/13/29
Prepare Operations	1 mon	6/13/29
Prepare Ground Sopport	1 mon	7/11/29
Reviews	40 days	8/8/29
ORR	1 mon	8/8/29
FRR	1 mon	9/5/29
Phase D Margin	3 mons	10/3/29

Figure 7 – Five Year Plan Based on NASA's Project Life Cycle (SHE 3.0)

19

2.10. Conclusion

Over the course of a year, PARSEC conducted multiple trade studies to iterate the system design to its current version. In April of 2024, the team's research culminated in an experiment testing the candidate additives, utilizing both alumina and Buildup #22 to determine the feasibility of regolith conglomeration.

From the 18 testing iterations, it was concluded that the Buildup #22 testing campaign yielded a perfect record of conglomeration and created a "landing pad" for all eight tests. Alumina, on the other hand, did not produce any solid landing pads, but did show evidence of conglomeration under a microscope. It is important to note that these experiments had limitations, such as being conducted in a pressured environment and with Earth's gravity field instead of the Moon's. Another significant limitation was the challenge of directly measuring and quantifying PSI reduction. High fidelity simulations and analysis could yield similar results supporting the hypothesis of a lander-scale replication of these tests. Ideally, tests would be conducted under more realistic conditions and employ better equipment for PSI measurements.

PARSEC's original proposal, when reviewed by the HuLC forum judges, returned some concerns. The team has since reassessed and is addressing these concerns. To address the concern that has to do with sufficient heat flux at the nozzle exit, recent testing has shown promising results indicating that with the right additive, conglomeration is achievable, although further at-scale testing is still required. Additional concerns centered on the additive's ability to provide adequate bonding and hardness to the surface. Tests using Buildup #22 on the LSP-2 lunar regolith simulant demonstrated strong bonding capability. Another concern is whether the resulting landing pad will be strong enough to support the lander plume loads. Static structural simulations conducted using a simplified landing pad model predict that a pad consisting of approximately a 50 wt% additive, like what was observed with the conglomeration tests, will survive the loads exerted by the landing.

Despite the success of the small-scale tests, further experimentation is necessary to overcome their limitations and determine its feasibility for the Artemis missions. This entails conducting numerical and experimental tests on larger scales, under accurate environmental conditions, and using different shapes and sizes of additives, such as spherical or larger particles. Furthermore, testing should involve more additive candidates, like SiAlON, Alumina, Zirconia, ZTA, and nickel alloys. If implemented by the Artemis Program, the results of these tests will aid in ultimately achieving the goal of effectively managing the risks posed by PSI in a cost-efficient and sensible manner.

Project PARSEC is confident in the proposed solution's ability to mitigate PSI via the use of a minimally invasive additive-deployment system near the lander's rocket nozzles to inject a granular ceramic or metal additive into the exhaust plume, which will form a solid coating on the lunar surface, protecting the landing site from erosion and ensuring success to future lunar exploration.

3. Appendix

Table 8 – Candidate Additive Selection Criteria

Criteria	Weight	Description
Safety	5%	An ideal additive should be non-toxic to humans and should not compromise the safety of any astronauts on the lander or the lunar surface.
Plume Survivability	20%	An ideal additive should be able to perform optimally within the high temperatures of the lander plume.
Lunar Environment Survivability	20%	An ideal additive should be able to perform optimally when deposited on the lunar surface and when exposed to the near-vacuum environment of the Moon.
Portability	10%	An ideal additive should be easy to store and transport on the lunar lander for the purpose of transit and deployment.
Technology Readiness Level (TRL)	10%	An ideal additive should have been used for a similar application in the past with demonstrated success.
Testability	15%	It should be possible for researchers to design and test an ideal additive's functionality within the constraints of their budget and timeline.
Accessibility	10%	An ideal additive should be easy for researchers to obtain within the constraints of their budget and timeline.

Table 9 – Mitigation Methods Trade Study

Mitigation Methods			Scores	Trades						
Criteria	Mandatory? (Y=1/ N=0)	Weight	Scale	Deployable Landing Pad (Cargo Drop)	Landing Boosters at top	Ballistic Landing	Electrically Charged Soil	Change Shape and Angle of plume	Exhaust Additive to create Landing Pad	Melt Regolith from Lander
Modifications Required	0.5	8%	1-3	2.5	1	2	2.5	1.5	2.5	2.5
Current Understanding	0	10%	1-3	3	2	3	1	1.5	2	1.5
Available Information	1	5%	1-3	2.5	3	2.5	2	1.5	2.5	2
Reusability	0	5%	1-3	3	3	2	3	2.5	3	3
TRL	0	5%	1-3	1	2.5	3	1	1	1	1
Mass	0	15%	1-3	1	2	3	3	3	3	3
Volume	0	8%	1-3	1	3	3	3	3	3	3
Cost	0	8%	1-3	1	2	2	2.5	2	2.5	1
Power	0	5%	1-3	3	3	3	2	3	3	1
Effectiveness	0	8%	1-3	3	2	3	1.75	1	2	2.5
Complexity	0	8%	1-3	1	2	3	1.5	2	2	1
Safety	1	15%	1-3	3	2	1	3	2.5	3	1
Weighted Total %		100%		69%	73%	82%	77%	71%	85%	63%

Table 10 – Candidate Additives Trade Study

Plume Additive			Scores	Trades					
Criteria	Mandatory? (Y=1/ N=0)	Weight	Scale	Ceramics	Thermoplastics	SiAlON Thermal Spray	Liquid Nitrogen	Lotus Leaf	Acids
Safety/non-toxic	1	5%	1-3	3	3	3	3	3	2
Plume Survivability (Temp, Press.)	1	20%	1-3	3	1.5	3	1	2	2
Lunar Environment Survivability	1	20%	1-3	3	2	3	1	3	2
Transit/Deployment	0	10%	1-3	3	3	2.75	1.5	3	1
TRL	0	10%	1-3	2	2	1.25	3	3	1
Testability	0	15%	1-3	2	2.5	2	3	3	1.5
Effectiveness	0	10%	1-3	2.5	1.5	2	1.75	1.5	1.5
Accessibility of Additive	0	10%	1-3	3	3	3	3	1	3
Weighted Total %		100%		90%	73%	85%	64%	82%	59%

Table 11 – Deployment Systems Trade Study (Powder)

Deployment System				Scores		Trades								
Criteria	Mandatory? (Y=1/ N=0)	Weight	Scale	Thermite Microcapsules*	Auger	Impeller	Extra Engine	Cannon	Magazine	Fluidization	COPVs *	Ionization Fluidizatoin *
Modifications Required	1	15%	1-3	3	2	2	1	2	2	2	2	2
Plume Survivability (Temp, Press.)	1	20%	1-3	1.5	3	3	3	2	2.5	3	3	3
Danger to Vessel	1	10%	1-3	1.5	3	2.5	1	3	2.5	3	3	3
Transit/Weight	1	10%	1-3	3	2	1.5	1	3	2	2.5	2.5	2.5
TRL	0	10%	1-3	2	2	3	3	2	1	3	3	3
Testability	0	15%	1-3	2	1.5	3	1	3	1	3	3	3
Effectiveness	1	10%	1-3	2.5	1	3	1.5	1.75	1	3	3	3
Resource Consumption	1	10%	1-3	3	1.5	1.5	1.5	3	3	2.5	2.5	2
Weighted Total %		100%		75%	69%	83%	57%	81%	63%	92%	92%	90%

*Can be integrated with other deployment systems

Table 12 – Risk Summary

Risk Number	Severity	Description	Mitigation Plan
1	RED	Additive does not adhere the lunar regolith to form a solid coating (Chemical, Technical Performance, Operational)	Perform tests to gather empirical data to prove that the expected reactions will occur.
2	RED	System mass is too high to be practical (Technical Performance, Operational)	Reduce system mass by using an additive with less mass, choosing a deployer design with less mass, or find other ways to reduce the system mass.
3	RED	Landing pad is destroyed by the force of the lander's plume (Technical Performance, Operational)	Ensure analytically that the landing pad will have a high enough strength to withstand the maximum pressure of the plume for as long as necessary (Section 2.6.3). This can be accomplished by selecting an additive that can meld with the regolith to form a high-strength composite ceramic or cermet and ensuring that the additive is evenly distributed across the surface beneath the lander.
4	YELLOW	Additive does not melt in the plume, due to either additive properties or variable plume thermal dynamics (Thermal, Technical Performance)	Simulate the injection of the additive into plumes of increasing heat and analyze the pads created to determine how well the additive melted at those temperatures.
5	RED	Additive melts too much/gets vaporized in the heat of the plume (Thermal, Operational)	Like risk 4, but ensure the heats increase enough to create a factor of safety to make sure the plume is not too hot for the additive.
6	YELLOW	Additive does not fluidize in the deployer (Operational)	Test different sized additive particles with different fluidization methods to find which method and which sizes work best together. Once the optimal system is found, test it for reliability in a vacuum, low gravity environment.
7	YELLOW	Additive cost is expensive in large quantities (Cost, Supportability)	According to ANSYS®, Inc. in Figure 23, Aluminum Nitride will have the highest budgetary impact at around 135 $/kg, making Sialon formation the most expensive option. Most other additives cost around 25 $/kg. For budgetary purposes, selecting a lesser performing additive may bring the use cost down.
8	GREEN	Additive poses health hazard to workers before launch (Safety, Regulations, Programmatic)	Implement administrative and engineering controls, such as fume hoods and proper PPE, to ensure that all workers are safe from possible health hazards posed in the additive's Safety Data Sheet (Space Resource Technologies, 2021) (GNPGraystar, 2020).

9	GREEN	Leftover additive can pose as a health hazard to astronauts (Safety, Liability)	The additive will be composed of some of the same materials contained in the lunar regolith, such as Alumina (Space Resource Technologies, 2023), therefore would not pose any additional hazard to the astronauts. However, decommissioning plans could include removal and disposal of any landing pad remnants as to protect the astronauts from further contact.
10	GREEN	Deployers structures and materials could fail under the conditions of spaceflight and the space environment (Operational)	Run multiple simulations, testing thermal conditions, performing finite element analysis, then conduct tests with a prototype structure to ensure its integrity.
11	YELLOW	Deployer mechanical mechanisms fail to actuate (Technical Performance, Operational)	Ensure that each fluid control and fluidization component can safely function in the lunar environment, then simulate the system functioning reliably in conditions like that of the lunar environment.
12	GREEN	Metal components of the deployer cold-weld together (Operational)	Research must be done on structural designs' vulnerabilities to cold welding to determine if the current design is at risk of cold-welding, and how to reiterate if it is at risk.
13	GREEN	Pressure within the deployment system is not strong enough to fluidize and eject the additive (Operational)	Conduct testing of the deployment system with pressures below and above optimal to determine the safety range of pressures, and ensure the system is designed to stay within that range.
14	YELLOW	Deployment system does not eject all the additive, has low efficiency (Operational)	Simulations and testing must be done to determine if deployer will eject all the additive.
15	YELLOW	Within fluid tanks, slosh dynamics behave differently than expected (Operational)	Research must be done to determine if slosh dynamics poses a threat to the mission.
16	GREEN	Not all the injected additive makes it into the plume (Operational, Liability)	Simulations and testing must be done to determine if the angling and distance of the deployer ejects all the additive into the plume.
17	YELLOW	Conglomerated chunks kicked up by plume cause more damage to lander or surrounding assets than PSI (Operational)	Conduct tests to determine what shapes and sizes of conglomerated chunks may form during the deployment process. Reduce the likelihood of these chunks being kicked up at high speeds by experimenting with different additives and changing how the additive is distributed into the plume.

Table 13 – PARSEC Testing Campaign

Test Number	Surface Composition	Additive	Height (from attachment start)	Duration (approx.) (s)	Notes
Test 1 (Day 1)	Nothing	None	9 pegs	44s	Box Integrity Lessened
Test 2	Sand	None	16 pegs	25s	Torch too high
Test 3	Sand	Buildup #22	unknown	35s	Conglomeration Success
Test 4	Sand	Buildup #22	10 pegs	37s	Conglomeration Success
Test 5	Regolith	Alumina	13 pegs	34s	No Conglomeration
Test 6	Regolith	Alumina	13 pegs	36s	No Conglomeration
Test 7 (Day 2)	Regolith	Alumina	13 pegs	36s	No Conglomeration
Test 8	Regolith	Alumina	11 pegs (5.5 in. to surface)	39s	No Conglomeration
Test 9	Regolith	Alumina	9 pegs (4 in. to surface)	40s	Minor conglomeration
Test 10	Regolith	Alumina	10 pegs	37s	Additive Clog, No conglomeration
Test 11	Fire Brick	Alumina	10 pegs	71s	Additive Clog, No conglomeration
Test 12	Fire Brick	Buildup #22	10 pegs	23s	Conglomeration Success
Test 13	Regolith	Buildup #22	unknown	44s	Conglomeration Success
Test 14	Regolith	Buildup #22	unknown	~30s	Conglomeration Success
Test 15	Regolith	Buildup #22	unknown	~30s	Conglomeration Success
Test 16	Regolith	Buildup #22	unknown	~30s	Conglomeration Success
Test 17	Regolith	Buildup #22	12 pegs	60s	Conglomeration Success
Test 18	Regolith	Alumina	11 pegs	60s	No Conglomeration
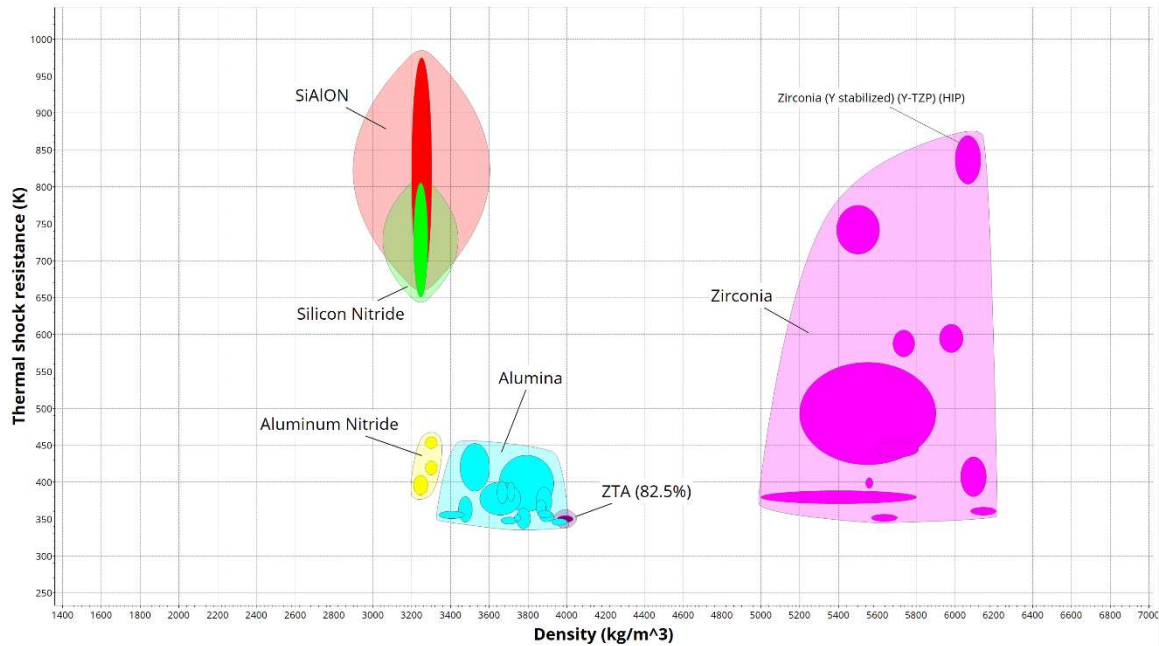
Figure 8 – Thermal Shock Resistance of Relevant Technical Ceramics (ANSYS®, Inc.)
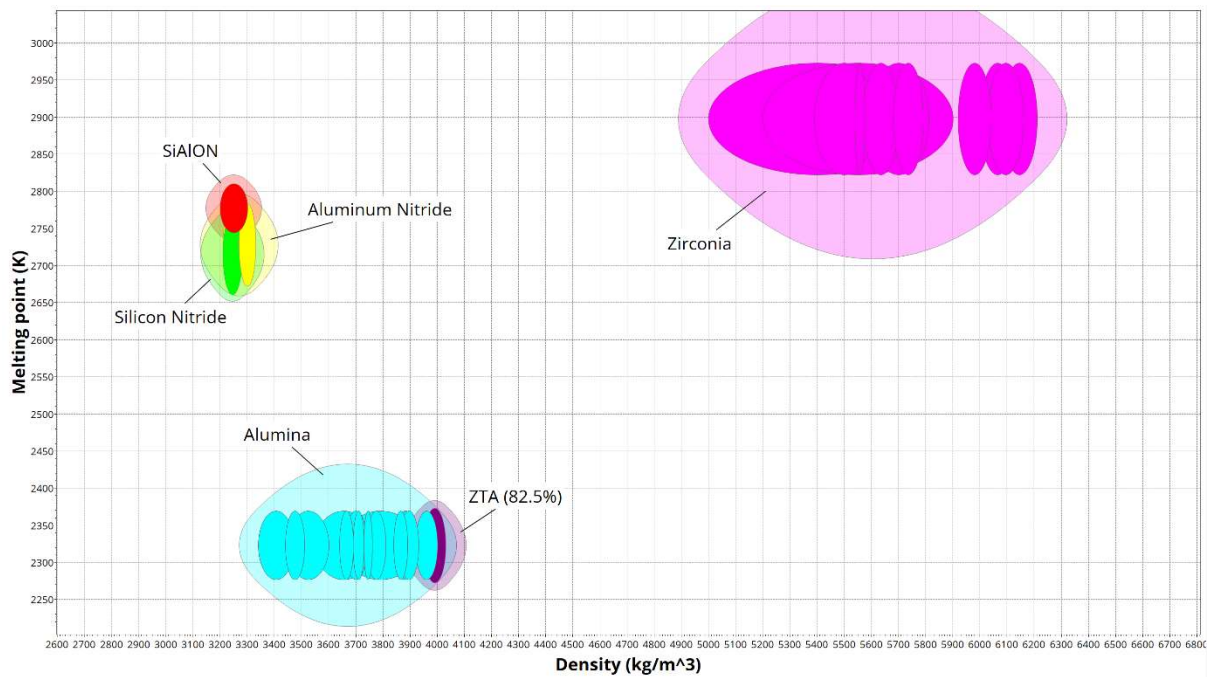
Figure 9 – Melting Point of Relevant Technical Ceramics (ANSYS®, Inc.)
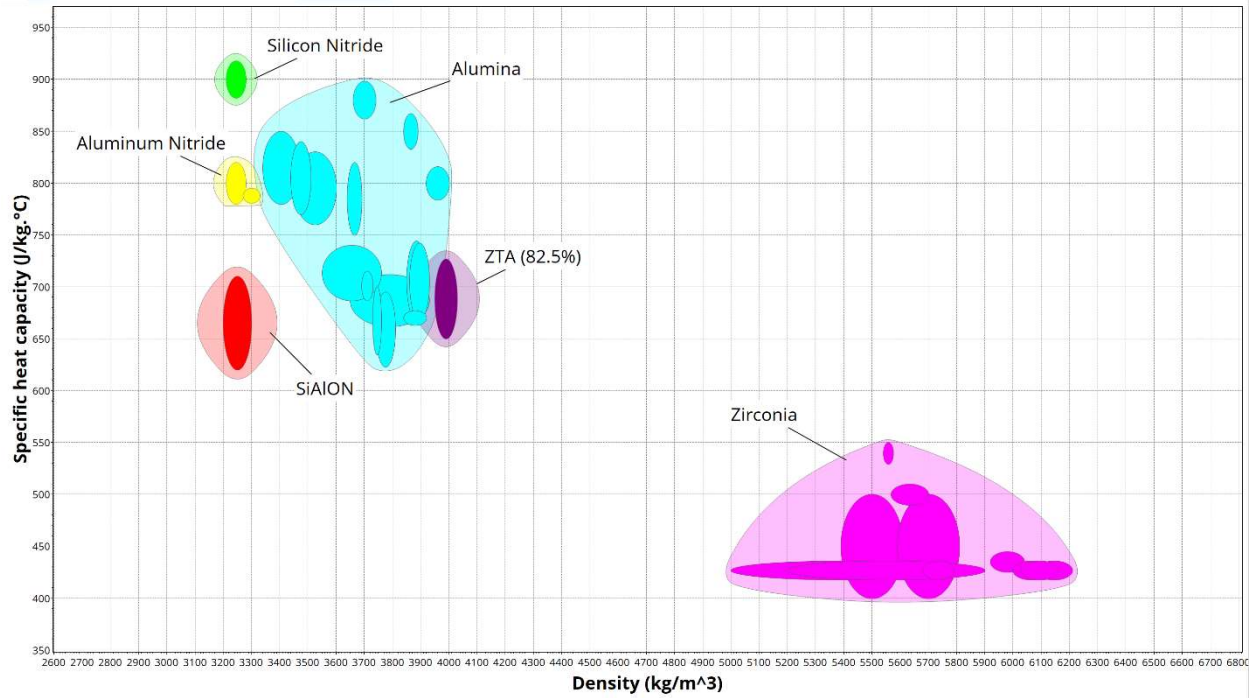
Figure 10 – Specific Heat Capacity of Relevant Technical Ceramics (ANSYS®, Inc.)
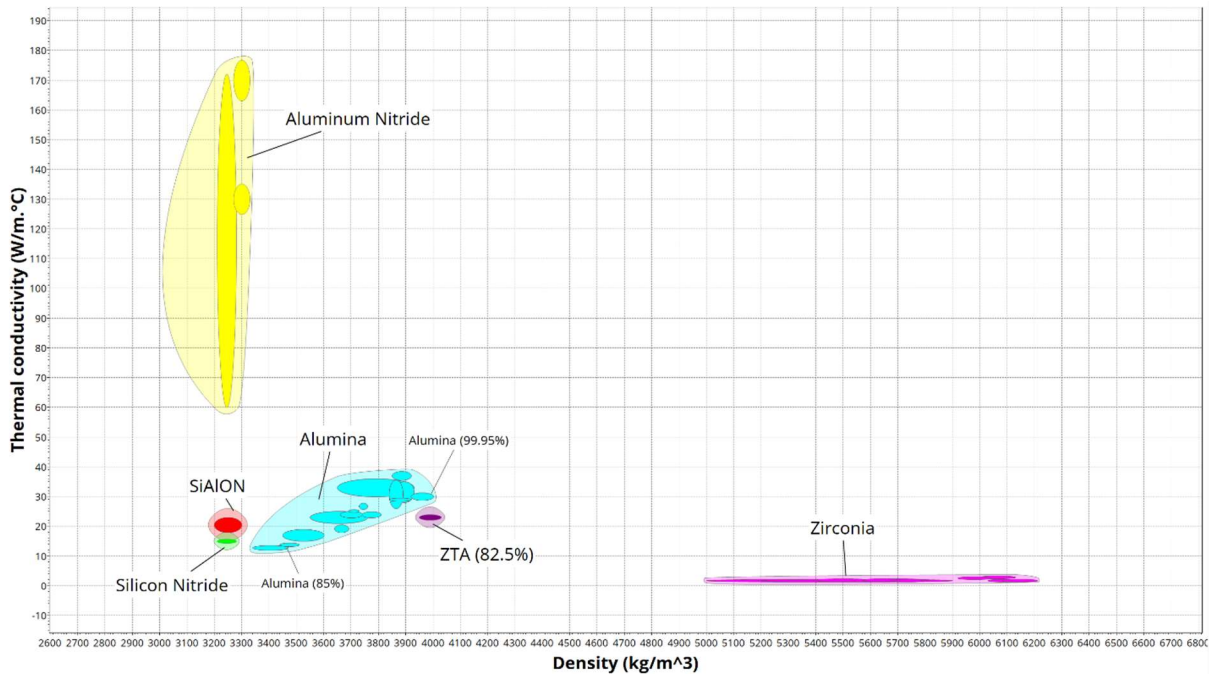
Figure 11 – Thermal Conductivity of Relevant Technical Ceramics (ANSYS®, Inc.)
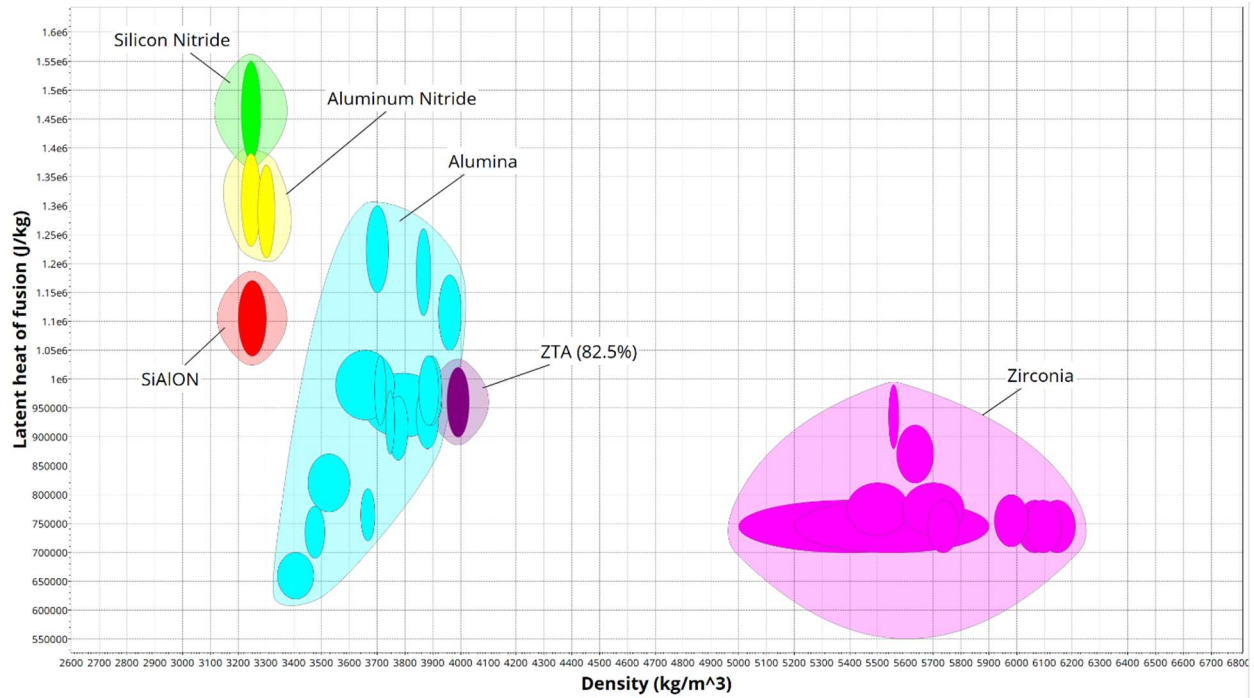
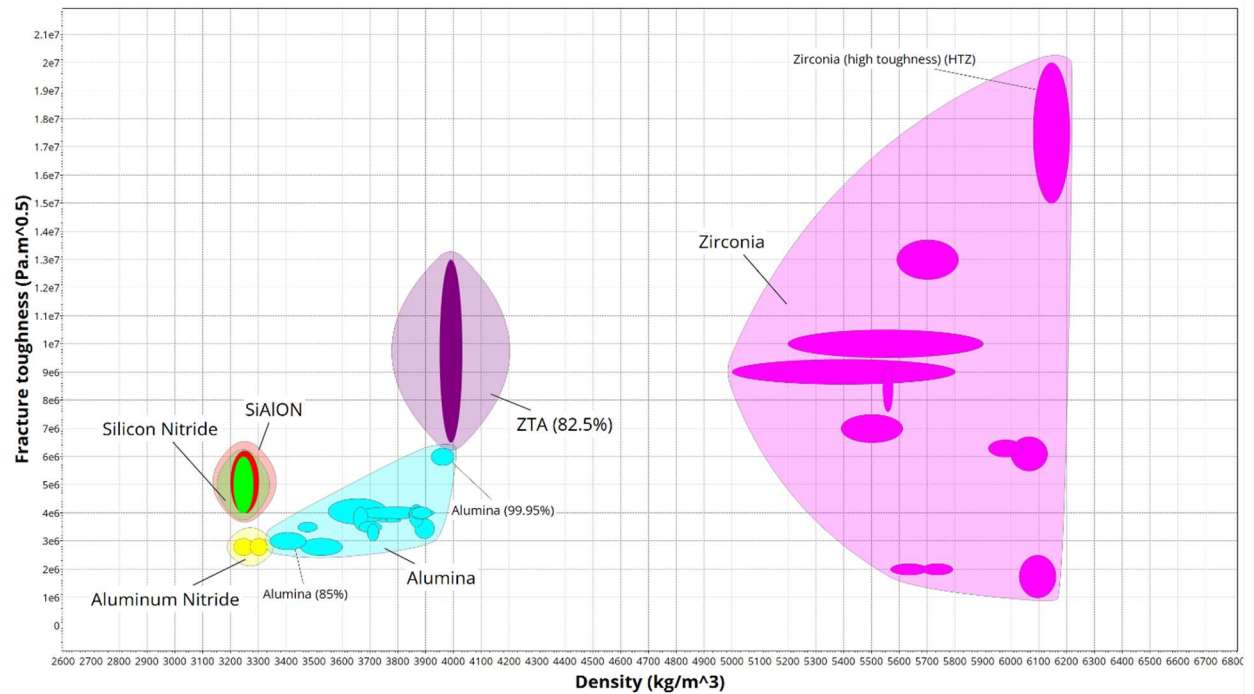**Figure 12 – Latent Heat of Fusion of Relevant Technical Ceramics (ANSYS®, Inc.)**

Figure 13 – Fracture Toughness of Relevant Technical Ceramics (ANSYS®, Inc.)
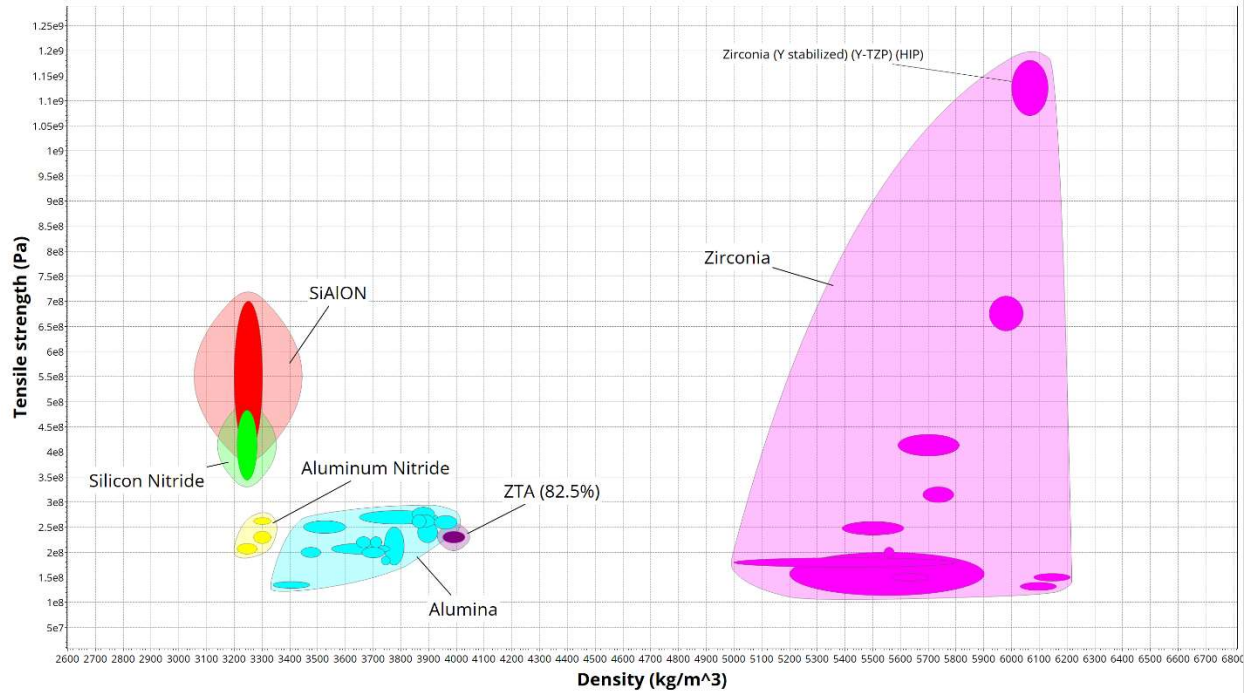
Figure 14 – Tensile Strength of Relevant Technical Ceramics (ANSYS®, Inc.)
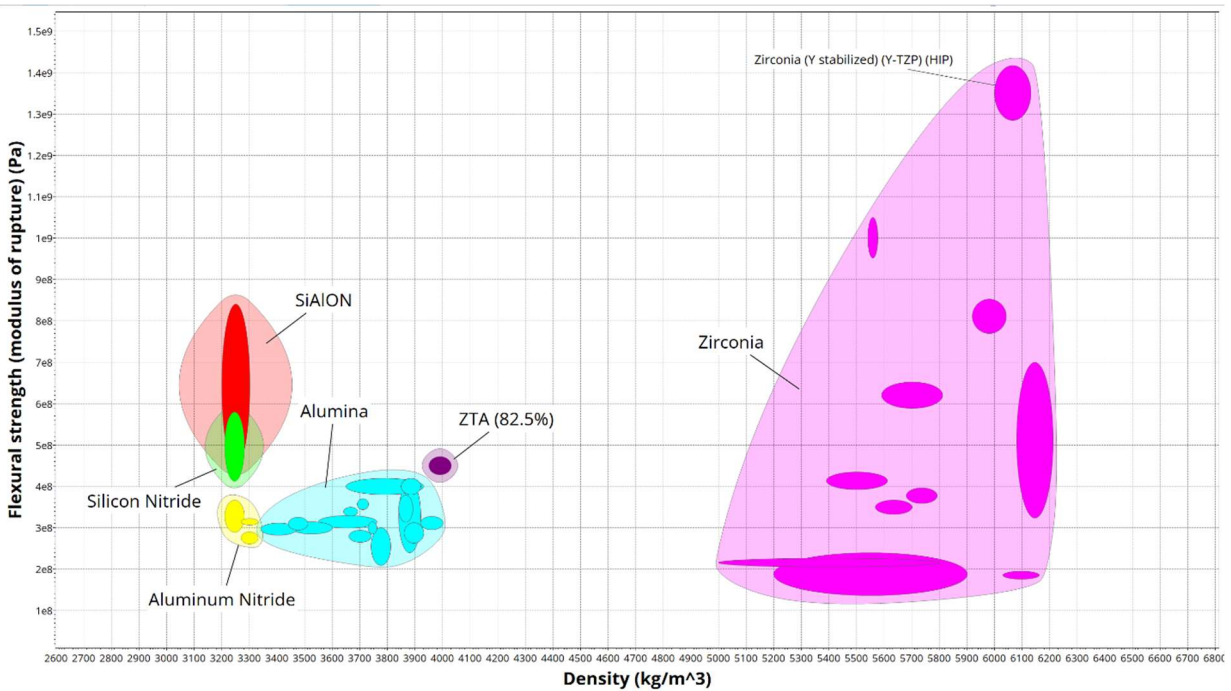
Figure 15 – Flexural Strength of Relevant Technical Ceramics (ANSYS®, Inc.)

28
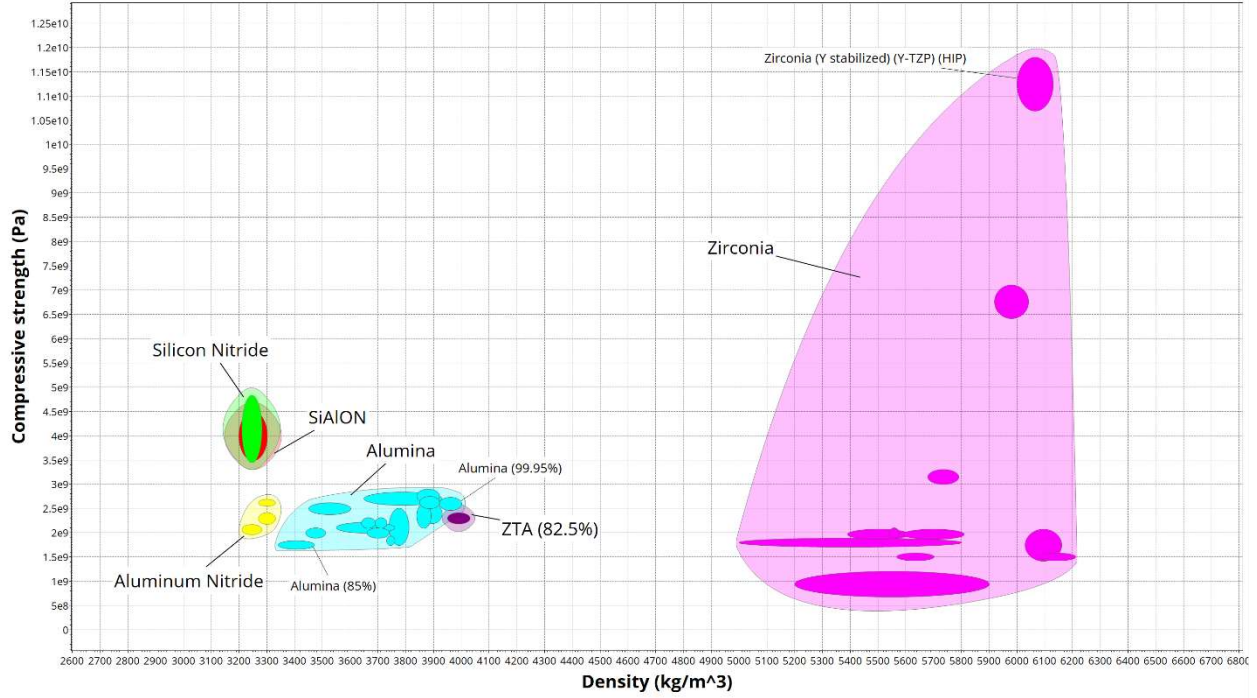
Figure 16 – Compressive Strength of Relevant Technical Ceramics (ANSYS®, Inc.)
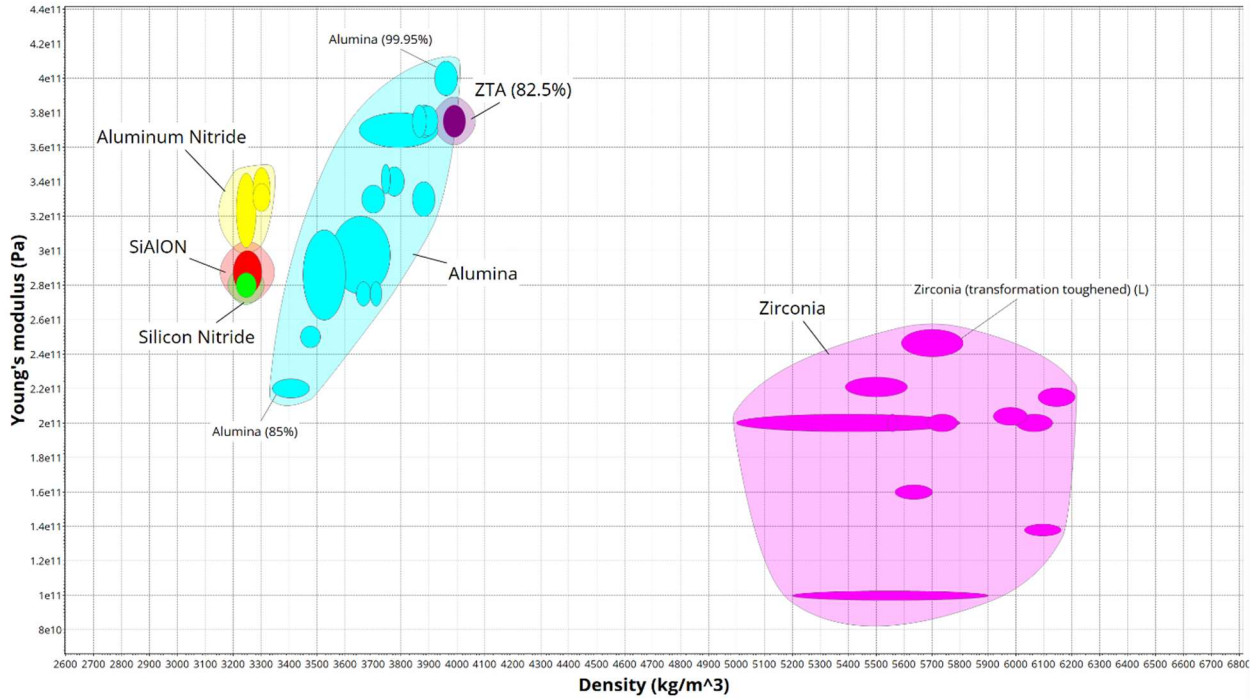
Figure 17 – Young's Modulus of Relevant Technical Ceramics (ANSYS®, Inc.)
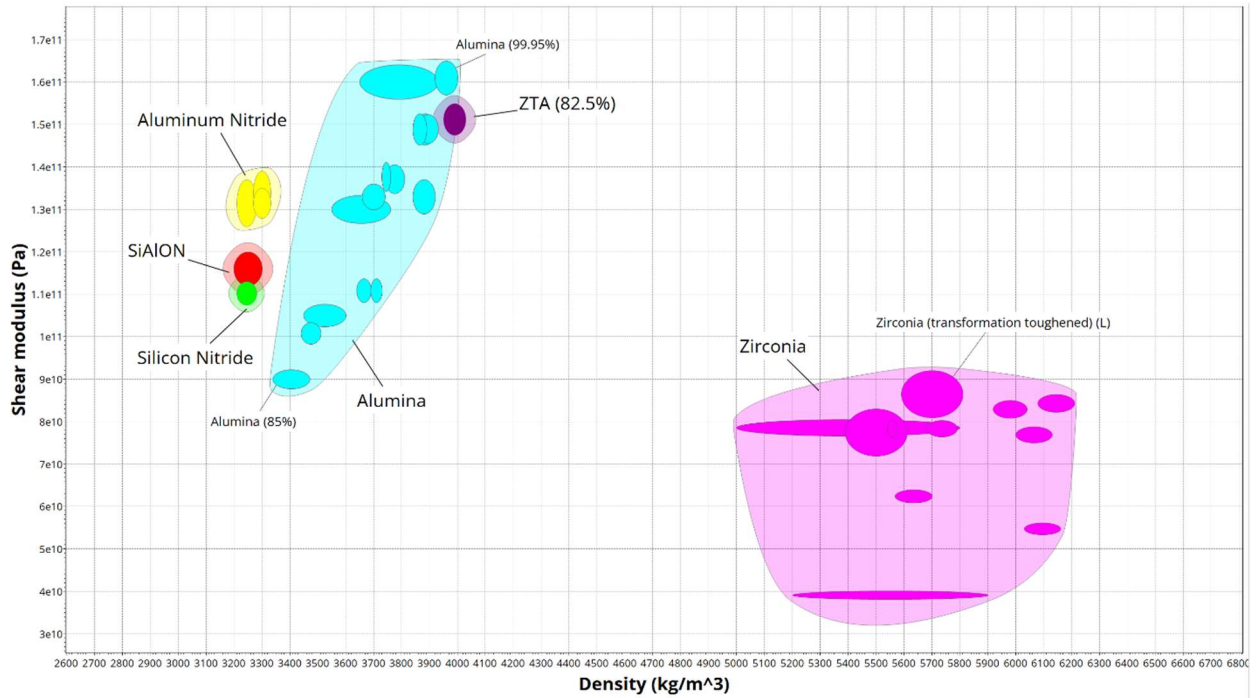
Figure 18 – Shear Modulus of Relevant Technical Ceramics (ANSYS®, Inc.)
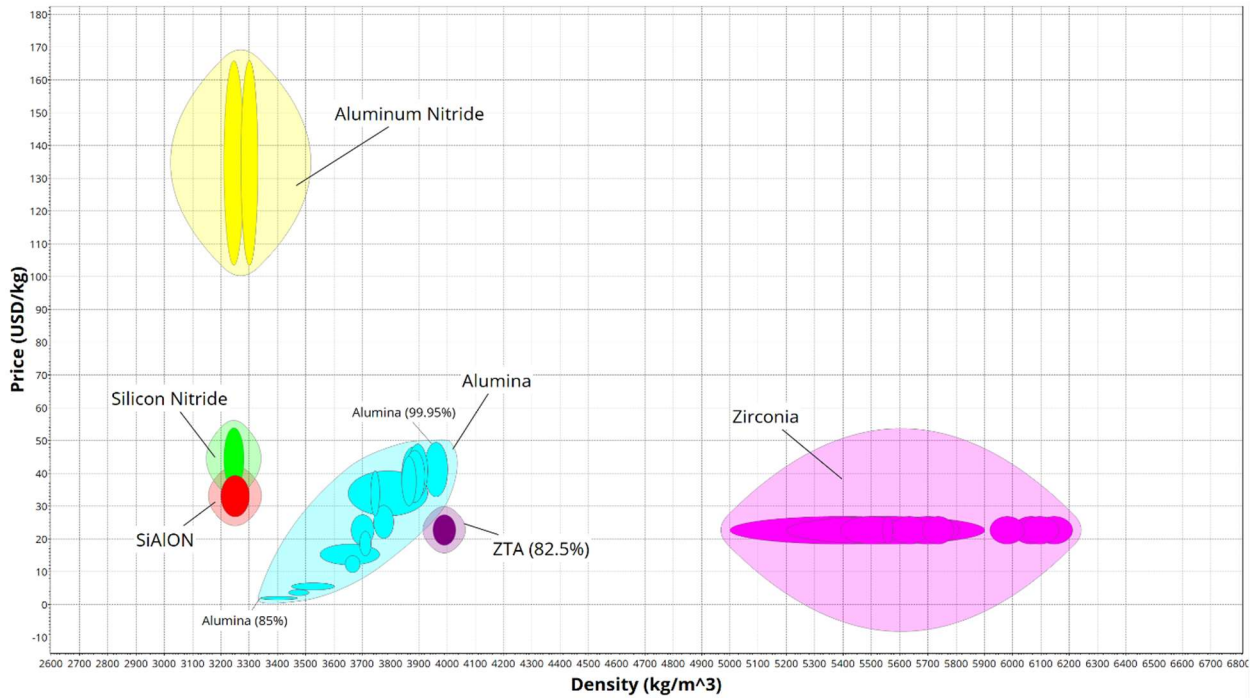
Figure 19 – Prices of Relevant Technical Ceramics (ANSYS®, Inc.)
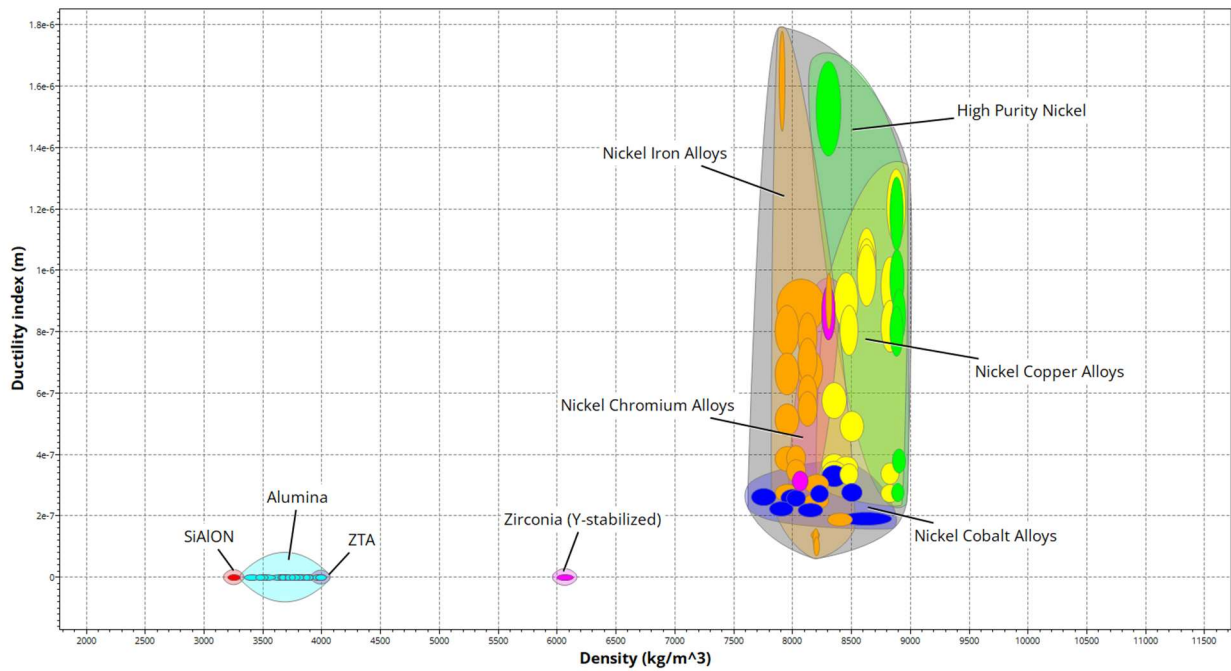
Figure 20 – Ductility Indexes of Candidate Additives (ANSYS®, Inc.)
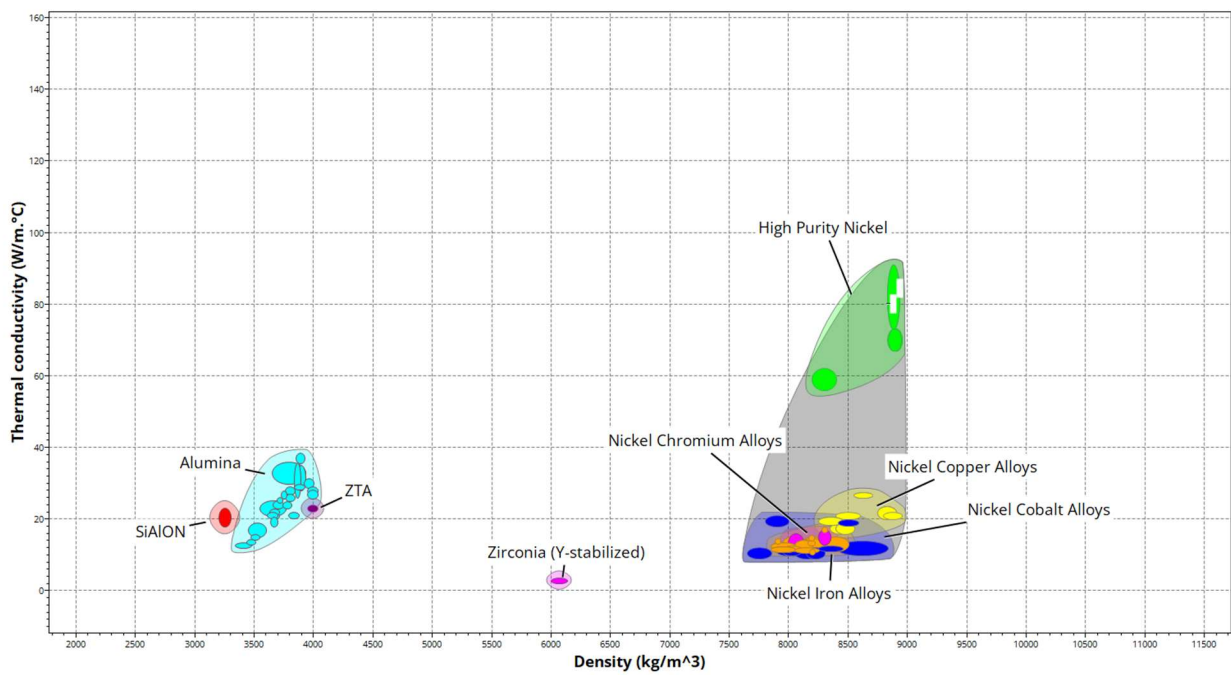
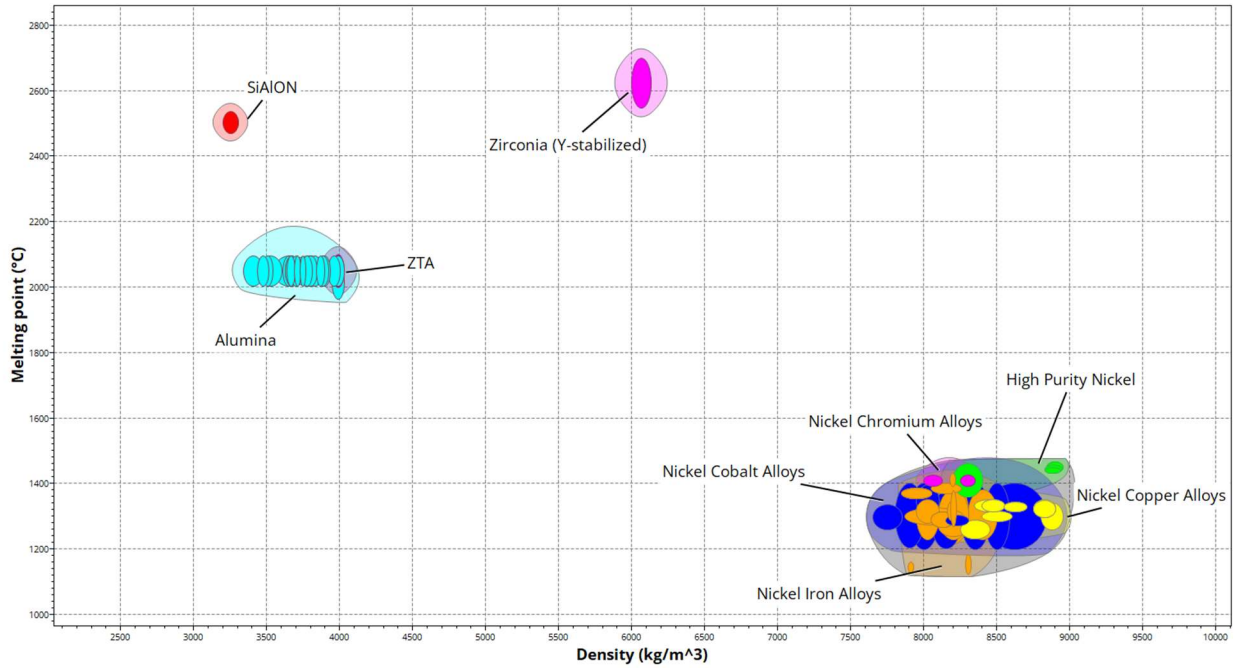**Figure 21 – Thermal Conductivity of Candidate Additives (ANSYS®, Inc.)**

31

Figure 22 – Melting Point of Candidate Additives (ANSYS®, Inc.)
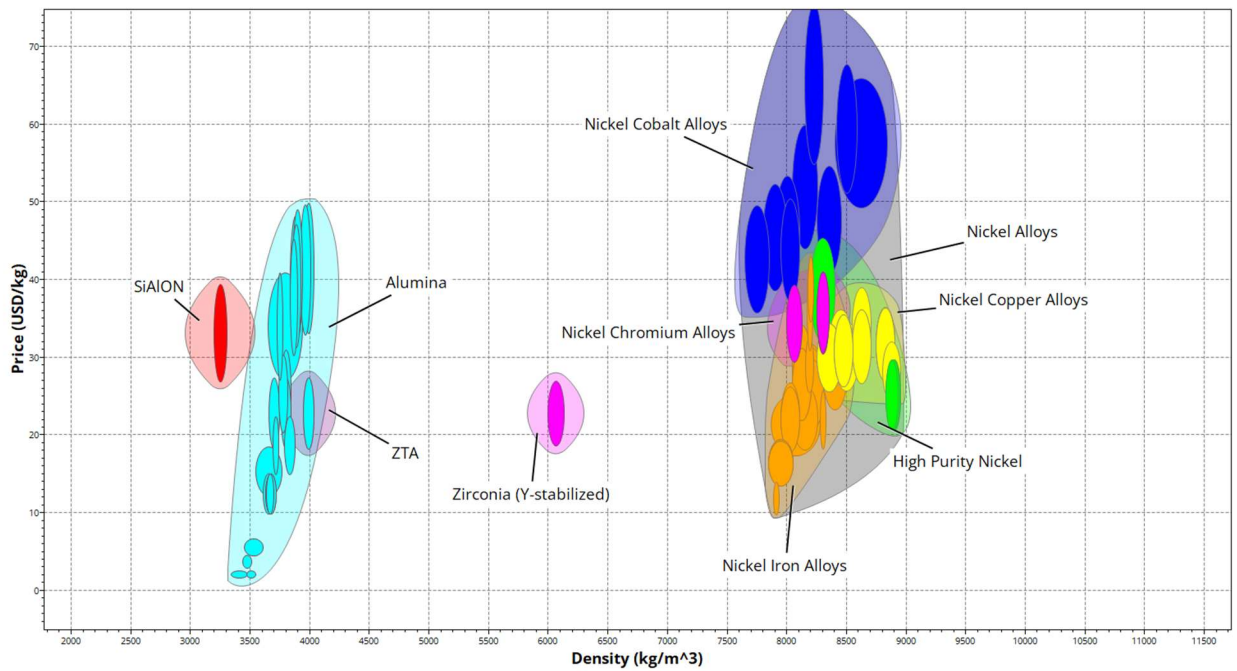

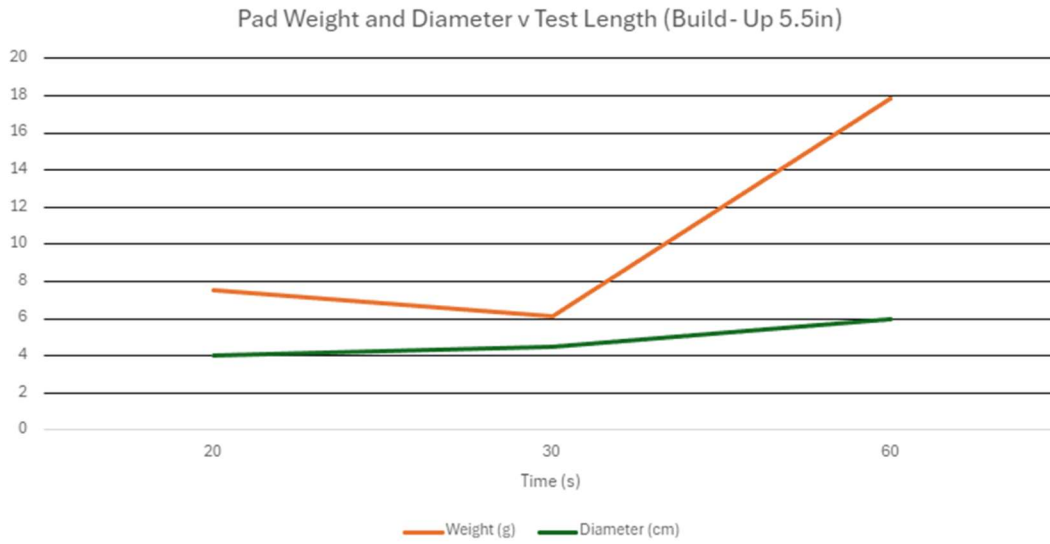**Figure 23 – Prices of Candidate Additives (ANSYS®, Inc.)**
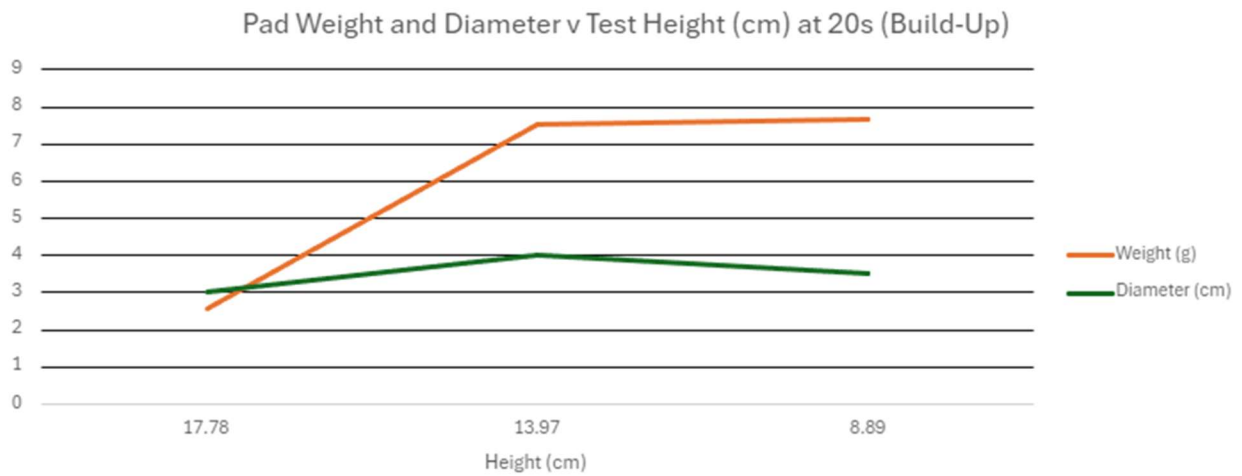
Figure 24 – Pad Weight and Size over Test Length
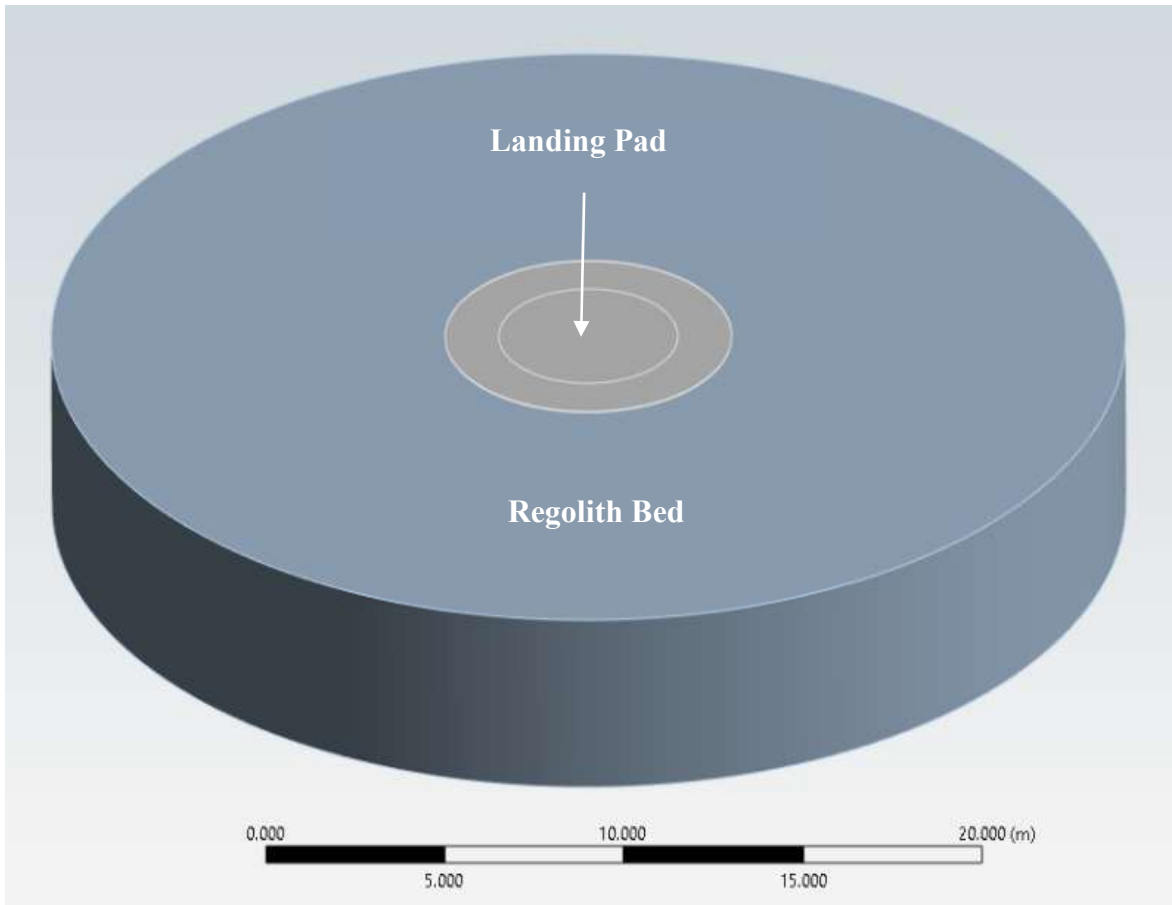

Figure 25 – Pad Weight and Size over Test Height

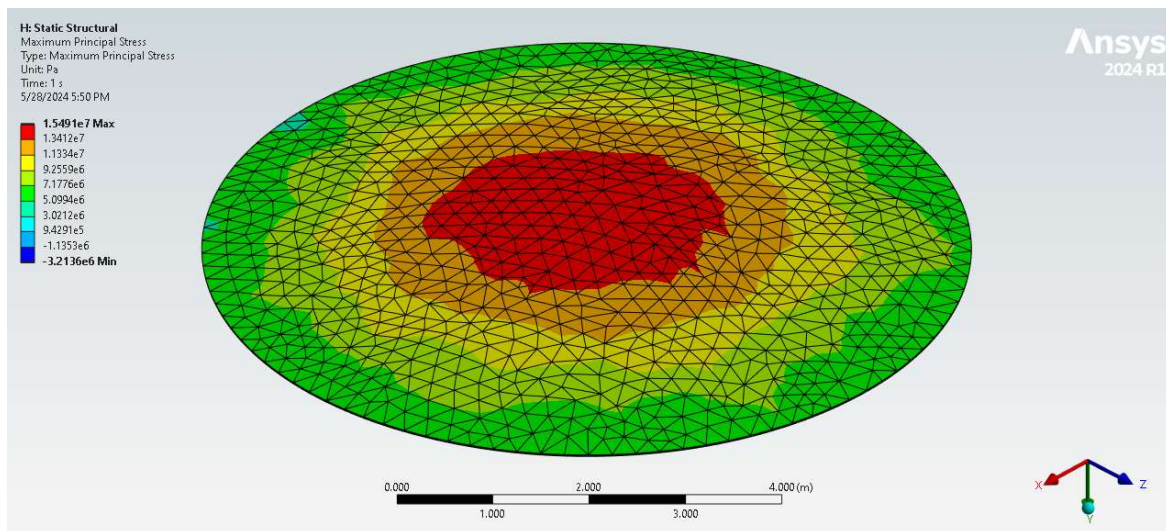**Figure 26 – Landing Pad Simulation Geometry (ANSYS, Inc.)**

Figure 27 – 8m 2cm Landing Pad Underside Maximum Principal Stress Plot (ANSYS, Inc.)

Table 14 – Material Properties for Composite Property Calculations

Material	Density (g/cm^3)	Elastic Modulus (GPa)	Tensile Strength (MPa)
Anorthosite	2.2	70	10
Alumina	3.9	370	250
Zirconia	6.0	200	1100
ZTA	4.0	370	220
SiAlON	3.3	300	400
Nickel Alloy	8.9	150	450

Volume Fractions:

$$wt\%_{additive} = \frac{m_{additive}}{m_{pad}} = \frac{\rho_{additive}V_{additive}}{\rho_{pad,avg}V_{pad}} = \frac{\rho_{additive}}{\rho_{pad,avg}}v_{additive}$$

$$\Rightarrow v_{additve} = \frac{\rho_{pad,avg}}{\rho_{additive}}wt\%_{additive}$$

$$\Rightarrow v_{anorthosite} = \frac{\rho_{pad,avg}}{\rho_{anorthosite}}wt\%_{anorthosite} \tag{7}$$

Average Landing Pad Density:

$$v_{additive} + v_{anorthosit} = 1$$

$$\Rightarrow \frac{\rho_{pad,avg}}{\rho_{additive}}wt\%_{additive} + \frac{\rho_{pad,avg}}{\rho_{anorthosite}}wt\%_{anorthosite} = 1$$

$$\Rightarrow \rho_{pad,avg} = \frac{\rho_{additive}\rho_{anorthosite}}{\rho_{anorthosite}wt\%_{additive} + \rho_{additive}wt\%_{anorthosite}} \tag{8}$$

Landing Pad Mass:

$$m_{pad} = \rho_{pad,avg}V_{pad}$$

$$\Rightarrow m_{pad} = \frac{\rho_{additive}\rho_{anorthosite}V_{pad}}{\rho_{additive}wt\%_{anorthosite} + \rho_{anorthosite}wt\%_{additive}} \tag{9}$$

Additive Mass:

$$m_{additive} = m_{pad}wt\%_{additive} \tag{10}$$

Table 15 – Landing Pad Simulation Parameters

Sim No.	Description/ Purpose	Bed Diameter (m)	Bed Depth (m)	Bed Element Size (m)	Bed Deformation Modulus (kPa)	Pad Diameter (m)	Pad Thickness (cm)	Pad Element Size (m)	Pad Elastic Modulus (GPa)	Applied Load (kN)	Load Type	Max Principal Stress (MPa)	Max Shear Stress (MPa)
1	Initial Simulation	30	5	0.5	100	15	5	0.25	100	65	Distributed, 5m Diameter	10.6	5.3
2	Large Bed Modulus	30	5	0.5	250	15	5	0.25	100	65	Distributed, 5m Diameter	7.2	3.6
3	Small Bed Modulus	30	5	0.5	10	15	5	0.25	100	65	Distributed, 5m Diameter	18.4	9.2
4	Large Pad Modulus	30	5	0.5	100	15	5	0.25	400	65	Distributed, 5m Diameter	16	8
5	Small Pad Modulus	30	5	0.5	100	15	5	0.25	10	65	Distributed, 5m Diameter	3.4	1.7
6	10cm Pad Thickness	30	5	0.5	100	15	10	0.25	100	65	Distributed, 5m Diameter	4.5	2.3
7	2.5cm Pad Thickness	30	5	0.5	100	15	2.5	0.25	100	65	Distributed, 5m Diameter	15.1	7.6
8	1cm Pad Thickness Fine	30	5	0.5	100	15	1	0.1	100	65	Distributed, 5m Diameter	11.4	6.2
9	1cm Pad Thickness Finer	30	5	0.5	100	15	1	0.05	100	65	Distributed, 5m Diameter	12.1	6.9
10	10m Pad Diameter	30	5	0.5	100	10	5	0.25	100	65	Distributed, 5m Diameter	10.7	5.4
11	10m Pad Dia, 2.5cm	30	5	0.5	100	10	2.5	0.25	100	65	Distributed, 5m Diameter	15.5	8
12	10m Pad Dia, 1cm	30	5	0.5	100	10	1	0.25	100	65	Distributed, 5m Diameter	8.8	6.4
13	10m Pad Dia, 1cm, Fine	30	5	0.5	100	10	1	0.1	100	65	Distributed, 5m Diameter	11.3	6.3
14	10m Pad Dia, 1cm, Finer	30	5	0.5	100	10	1	0.05	100	65	Distributed, 5m Diameter	12.1	6.9
15	Point Load	30	5	0.5	100	15	4	0.25	100	65	Point Load	41.7	21.8
16	8m Pad Dia, 2cm	30	5	0.5	100	8	2	0.25	100	65	Distributed, 5m Diameter	15.5	7.9

3.1. References

ANSYS®, Inc. *Ansys® GRANTA Selector™.* www.ansys.com/materials.

ANSYS®, Inc. *Ansys® Mechanical™.* https://www.ansys.com/products/structures/ansys-mechanical

AZO Materials (2024). https://www.azom.com/

Cañas, E., Benavente, R., Borrell, A., Dolores Salvador, M. (2023). *Deposition of Advanced Ceramic Coatings by Thermal Spraying.* IntechOpen. https://doi.org/10.5772/intechopen.1002921

Clegg-Watkins, R. N., Jolliff, B. L., Boyd, A., Robinson, M. S., Wagner, R., Stopar, J. D., Plescia, J. B., & Speyerer, E. J. (2016, June 15). *Photometric characterization of the Chang'e-3 landing site using LROC NAC images*. Science Direct. https://www.sciencedirect.com/science/article/pii/S001910351500562X

Cocco, R., Reddy Karri, S. B., & Knowlton, T. (2014). *Introduction to Fluidization*. In AIChE. https://www.aiche.org/sites/default/files/cep/20141121.pdf#:~:text=Particles%20become%20fluidized%20when%20an%20upward-flowing%20gas%20imposes

Delgado, A., Shafirovich, E. (2013). *Towards better combustion of lunar regolith with magnesium.* Science Direct. Vol. 160, Issue 9, pp. 1876-82. https://www.sciencedirect.com/science/article/abs/pii/S0010218013001090

Exolith Labs (Space Resource Technologies) (2023). *Exolith Lunar Simulants Constituent Report.* https://cdn.shopify.com/s/files/1/0398/9268/0862/files/Lunar_Constituent_Report_Dec_2023.pdf?v=1703170361

Fan, X. (2021, July 19). *Nitrogen species in a thermal plasma under very low pressure (150 PA): Application to reactive plasma spraying.* Ceramics International. https://www.sciencedirect.com/science/article/pii/S0272884221022203

Faierson, Eric J., et. al. (2010). *Demonstration of concept for fabrication of lunar physical assets utilizing lunar regolith simulant and a geothermite reaction.* Acta Astronautica. https://www.sciencedirect.com/science/article/abs/pii/S0094576509005918

Fontes D., Mantovani J., Metzger P. (2022). *Numerical estimations of lunar regolith trajectories and damage potential due to rocket plumes.* Acta Astronautica. http://dx.doi.org/10.1016/j.actaastro.2022.02.016

Gates A., Jakubowski J., Regina A. (2023) *Nickel Toxicology.* National Library of Medicine.

German, R. M. (2003). *Sintering.* Encyclopedia of Materials: Science and Technology (Second Edition). https://doi.org/10.1016/B0-08-043152-6/01542-4

Gibson, I. A., Slim, C. J. S., Zheng, Y., Scott, S. A., Davidson, J. F., & Hayhurst, A. N. (2018, May 8). *An examination of Wen and Yu's formula for predicting the onset of fluidisation*. Science Direct. https://www.sciencedirect.com/science/article/pii/S0263876218302405

GNPGraystar, "*Calcined Alumina*," CAS 1344-28-1, 06/01/2020. Calcined Alumina, GNPGraystar: 37 John Glenn Dr. Amherst, NY 14228, 06/01/2020, https://gnpgraystar.com/wp-content/uploads/2020/10/Calcined-Alumina-2020.pdf

Hall, Loura (2021, April 08). *Regolith Adaptive Modification System (RAMs) to Support Early Extraterrestrial Planetary Landings (and Operations)*. NASA. https://www.nasa.gov/general/regolith-adaptive-modification-system-rams-to-support-early-extraterrestrial-planetary-landings-and-operations/

Immer C., Metzger P., Hintze P., Nick A., Horan R. (2010). *Apollo 12 Lunar Module exhaust plume impingement on Lunar Surveyor III*. Icarus. https://doi.org/10.1016/j.icarus.2010.11.013

International Syalons. (2021). *What are Sialon Ceramics?* https://www.syalons.com/resources/articles-and-guides/sialons/

Kaczmarek, M., Mariniak, M., & Szczucinska, A. (2019, October 3). *Experimental studies and modelling of the fluidization of sands*. Journal of Hydrology. https://www.sciencedirect.com/science/article/pii/S0022169419309400

Korzun, A., & Mehta, M. (2021, July 8). *Plume-Surface Interaction: Maturing Predictive Environments for Propulsive Landing on the Moon and Mars*. Ntrs.nasa.gov. https://ntrs.nasa.gov/citations/20210018148

Latka, Pawlowski, Winnicki, Sokolowski, Malachowska, Kozerski (2020). *Review of Functionally Graded Thermal Sprayed Coatings*. MDPI. https://doi.org/10.3390/app10155153

Li G., Helms E. J., Pang S. (2001) *Analytical Modeling of Tensile Strength of Particulate-Filled Composites*. Polymer Composites. http://dx.doi.org/10.1002/pc.10562

MacKenzie, K. J. D. (2000). *Effect of MgO, Y_2O_3, and Fe_2O_3 on silicothermal synthesis and sintering of X-sialon. an XRD, multinuclear MAS NMR and 57fe Mössbauer study.* Journal of the European Ceramic *Society*. https://www.sciencedirect.com/science/article/pii/S0955221900001096

Matchett, A. J. (2006). *Rotated, circular arc models of stress in silos applied to core-flow and vertical rat-holes*. ScienceDirect. https://www.sciencedirect.com/science/article/pii/S0032591005005565

McDANEL AMT. (2015). *Safety Data Sheet Sialon - McDanel Advanced Ceramic*. McDanel Advance Material Technologies. https://mcdanelceramics.com/wp-content/uploads/pdf/sds/SDS_McD_Sialon.pdf

Metzger P. T., Smith J., Lane J. E. (2011) *Phenomenology of soil erosion due to rocket exhaust on the Moon and the Mauna Kea lunar test site.* AGU. https://doi.org/10.1029/2010JE003745

NASA. (2021). *Project Cost Estimating Capability v2.3*. https://www.nasa.gov/ocfo/pcec-project-cost-estimating-capability/

NIA. (2023). *Mitigating Lunar Plume Surface Interaction (PSI) 2024 Proposal Guidelines*. Nianet; National Institute of Aerospace. https://hulc.nianet.org/wp-content/uploads/2023-HLS-Competition-Guidelines-FINAL.pdf

Sanpo, Wang (2013). *Feedstock Material Considerations for Thermal Spray*. ASM Handbook.
https://doi.org/10.31399/asm.hb.v05a.a0005727

Siperm (2024). *Fluidization and Discharge*. Tridelta Siperm® GMBH. (n.d.).
https://www.siperm.com/en/products/applications/bulk-material-handling/fluidization-and-discharge/

Space Resource Technologies, *"LSP-2 Lunar South Pole 2mm Simulant,"* 3/31/2021. LSP-2 Lunar South Pole 2mm Simulant, Space Resource Technologies: 532 S Econ Cir, Suite 100, Oviedo, FL 32765, 3/31/2021, https://cdn.shopify.com/s/files/1/0398/9268/0862/files/LSP-2_SDS_11_23_.docx.pdf?v=1700164729

Stanford Advanced Materials. *NN1868 Zirconia Toughened Alumina (ZTA) Nano Powder*.
https://www.preciseceramic.com/productsearch.html?search=ATZ

Turunen E., Hirvonen A., Varis T., Falt T., Hannula S., Sekino T., & Niihara K. (2007) *Application of HVOF Techniques for Spraying of Ceramic Coatings*. https://doi.org/10.2240/azojomo0260

Victor® (2010). *Material Safety Data Sheet*. MSCDirect.
https://www1.mscdirect.com/MSDS/MSDS00021/01388909-20110811.PDF

Watkins, R., Metzger, P. T., Mehta, M., Han, D., Prem, P., Sibille, L., Dove, A., Jolliff, B., III, D. P., Barker, D. C., Patrick, E., Kuhns, M., Laine, M., Radley, C. F. (2021). *Understanding and Mitigating Plume Effects During Powered Descents on the Moon and Mars.* Bulletin of the AAS, 53(4). https://doi.org/10.3847/25c2cfeb.f9243994

Yu, Z. (2014). *Sialons*. Ceramic-Matrix Composites. https://www.sciencedirect.com/science/article/pii/B978185573942050018X